

EW D-optimal Designs for Experiments with Mixed Factors

Siting Lin¹, Yifei Huang², and Jie Yang¹

¹University of Illinois at Chicago and ²Astellas Pharma, Inc.

May 23, 2025

Abstract

We characterize EW D-optimal designs as robust designs against unknown parameter values for experiments under a general parametric model with discrete and continuous factors. When a pilot study is available, we recommend sample-based EW D-optimal designs for subsequent experiments. Otherwise, we recommend EW D-optimal designs under a prior distribution for model parameters. We propose an EW ForLion algorithm for finding EW D-optimal designs with mixed factors, and justify that the designs found by our algorithm are EW D-optimal. To facilitate potential users in practice, we also develop a rounding algorithm that converts an approximate design with mixed factors to exact designs with prespecified grid points and the number of experimental units. By applying our algorithms for real experiments under multinomial logistic models or generalized linear models, we show that our designs are highly efficient with respect to locally D-optimal designs and more robust against parameter value misspecifications.

Key words and phrases: EW ForLion algorithm, Exact design, Mixed factors, Generalized linear model, Multinomial logistic model, Robust experimental design

1. Introduction

In this paper, we consider robust designs against unknown parameter values for experiments with discrete and continuous factors. A motivating example is the paper feeder experiment described in Joseph and Wu (2004). The goal was to ensure precise feeding of one sheet of paper each time to a copier. Two common failure modes are frequently observed, namely *misfeed* when the feeder fails to feed any sheet of paper, and *multifeed* when the feeder picks up more than one sheets of paper at a time. The experiment involves eight discrete control factors (see Table 2 in Joseph and Wu (2004) and also Section S4 in the Supplementary Material) and one continuous factor, the stack force. The responses fall into three mutually exclusive categories, namely *misfeed* (typically with low stack force), *normal*, and *multifeed* (typically with high stack force). The results of the original experiment were listed in Table 3 of Joseph and Wu (2004). The original design was conducted via a control array modified from $OA(18, 2^1 \times 3^7)$ (see Table 5 in

Joseph and Wu (2004)) for the eight discrete factors and an essentially uniform allocation on a predetermined set of discrete levels of the continuous factor. If a subsequent experiment will be conducted to study the factor effects, how can we do better?

In the original analysis by Joseph and Wu (2004), two generalized linear models (McCullagh and Nelder, 1989; Dobson and Barnett, 2018) with probit link were used to model `misfeed` and `multifeed` separately. However, since `misfeed` and `multifeed` do not occur simultaneously and are both possible outcomes of the experiment, it would be more appropriate to adopt one multinomial model rather than two separate binomial models, so that the factor effects can be estimated more precisely due to the combined data and also be comparable for different types of failures. In this study, we adopt the multinomial logistic models (Glonck and McCullagh, 1995; Zocchi and Atkinson, 1999; Bu et al., 2020) for analyzing the paper feeder experiment, which include baseline-category (also known as multiclass logistic), cumulative, adjacent-categories, and continuation-ratio logit models.

For experiments with discrete factors only, many numerical algorithms have been proposed for finding optimal designs, including Fedorov-Wynn (Fedorov, 1972; Fedorov and Hackl, 1997), multiplicative (Titterton, 1976, 1978; Silvey et al., 1978), cocktail (Yu, 2010), lift-one (Yang and Mandal, 2015; Yang et al., 2017; Bu et al., 2020), as well as classical optimization techniques (see Huang et al. (2024) for a review). According to Yang et al. (2016) and Huang et al. (2024), the lift-one algorithm outperforms commonly used optimization algorithms and obtains D-optimal designs with fewer distinct design points. For experiments with continuous factors only, Ai et al. (2023) incorporated the Fedorov-Wynn algorithm with the lift-one algorithm for continuation-ratio link models, Yang et al. (2013) and Harman et al. (2020) discretized the continuous factors into grid points and treated the experiments as with discrete factors.

For experiments with mixed factors, particle swarm optimization (PSO) algorithms have been applied for D-optimal designs under generalized linear models with binary responses (Lukemire et al., 2019) and cumulative logit models (Lukemire et al., 2022), which, however, cannot guarantee the optimal solution to be ever found (Kennedy and Eberhart, 1995; Poli et al., 2007). Huang et al. (2024) proposed a ForLion algorithm, which added a merging step to Ai et al. (2023)'s algorithm and significantly reduced the number of design points. In practice, it often leads to reduced experimental time and cost (Huang et al., 2024). Unlike PSO-types of algorithms, the ForLion algorithm is guaranteed to find D-optimal designs based on the general equivalence theorem (Kiefer, 1974; Pukelsheim, 1993; Atkinson et al., 2007; Stufken and Yang, 2012; Fedorov and Leonov, 2014).

The ForLion algorithm has been successfully applied to both generalized linear models and multinomial logistic models with mixed factors (Huang et al., 2024). However, it relies on pre-assumed parameter values and produces designs known as *locally optimal* (Chernoff, 1953), which may not be robust when the parameter values are misspecified. To address the limitation due to local optimality, Bayesian D-optimal designs have been proposed (Chaloner and Verdinelli, 1995), which maximize $E(\log |\mathbf{F}|)$ with respect to a prior distribution on unknown parameters, where \mathbf{F} is the Fisher information matrix associated with the design. However, a major drawback of Bayesian D-optimal designs is its computational intensity, even with D-criterion that maximizes the determinant of

the Fisher information matrix. As a promising alternative, Expected Weighted (EW) D-optimal designs have been proposed for generalized linear models (Yang et al., 2016), cumulative link models (Yang et al., 2017), and multinomial logistic models (Bu et al., 2020) with discrete factors, which maximize $\log |E(\mathbf{F})|$ or equivalently $|E(\mathbf{F})|$. Compared with Bayesian D-optimal designs, EW D-optimal designs are computationally much faster and often highly efficient in terms of the Bayesian criterion (Yang et al., 2016, 2017; Bu et al., 2020). Along this line, Tong et al. (2014) provided analytical solutions for certain cases of EW D-optimal designs for generalized linear models, and Bu et al. (2020) incorporated the lift-one and exchange algorithms with the EW criterion.

In this paper, we adopt EW D-criterion and adapt the ForLion algorithm for finding robust designs with mixed factors. The original EW D-optimal designs were proposed for experiments with discrete factors or discretized continuous factors. To solve our problems, we formulate in Section 2 the EW D-optimal criterion and characterize EW D-optimal designs for general parametric statistical models with mixed factors. In Section 3, we develop algorithms for finding two types of EW D-optimal designs with mixed factors, namely sample-based EW D-optimal designs for experiments with a pilot study, and integral-based EW D-optimal designs for experiments with a prior distribution for unknown parameters. We further formulate EW D-optimal designs for multinomial logistic models and generalized linear models, and propose an algorithm for converting approximate designs with mixed factors to exact designs with grid points, which is much faster than finding optimal designs restricted on the same set of grid points. In Section 4, we construct the proposed robust designs for two real experiments, namely the paper feeder experiment (Joseph and Wu, 2004), and an experiment on minimizing surface defects (Wu, 2008). In Section 5, we conclude our findings. The algorithms are implemented in R with version 4.4.2 and the simulations are run on a Windows 11 laptop with 32GB of RAM and a 13th Gen Intel Core i7-13700HX processor.

2. EW D-optimal Designs with Mixed Factors

Following Huang et al. (2024), we first consider experiments with a design region $\mathcal{X} = \prod_{j=1}^d I_j \subset \mathbb{R}^d$, where I_j is either a closed finite interval for the first k factors, or a finite set of distinct numerical levels for $k+1 \leq j \leq d$. In both cases, we denote $a_j = \min I_j > -\infty$ and $b_j = \max I_j < \infty$. If $k = 0$, all factors are discrete or qualitative; if $k = d$, all factors are continuous. Note that \mathcal{X} here is compact and built as a product of sets, which is common for typical applications.

For some applications, for examples, when the levels of some discrete factors are not numerical (see Example 1 below), or the level combinations of discrete factors under consideration are restricted to a true subset of all possible level combinations (see Example 2 below), we also need to consider design regions $\mathcal{X} = \prod_{j=1}^k I_j \times \mathcal{D}$, where $\mathcal{D} \subseteq \prod_{j=k+1}^d I_j$. Apparently, $\prod_{j=1}^d I_j$ is a special case of $\prod_{j=1}^k I_j \times \mathcal{D}$ with $\mathcal{D} = \prod_{j=k+1}^d I_j$.

Example 1. *A polysilicon deposition process for circuit manufacturing was described by Phadke (1989) involved one qualitative control factor, cleaning method (None for no cleaning, CM_2 for cleaning inside the reactor, and CM_3 for cleaning outside the reactor), and five other factors that are continuous in nature (see Table 4.1 in Phadke (1989)).*

Since the levels of cleaning method are not numerical, it would be more appropriate to convert it to two (binary) indicator variables ($\mathbf{1}_{CM_2}, \mathbf{1}_{CM_3}$) with $(0, 0), (1, 0), (0, 1)$ standing for None, CM_2 , and CM_3 , respectively. In this case, the corresponding design region is $\mathcal{X} = \prod_{j=1}^5 I_j \times \{(0, 0), (1, 0), (0, 1)\}$, where I_1, \dots, I_5 may be defined as in Table S1 of the Supplementary Material of Huang et al. (2024). Note that the cleaning method was simplified into a binary factor (CM_2 or CM_3) in Lukemire et al. (2022) and Huang et al. (2024). \square

Example 2. In the paper feeder experiment described by Joseph and Wu (2004), besides one continuous factor, there are eight discrete or qualitative control factors, including two binary ones and six three-level ones (see Section S4 in the Supplementary Material). Instead of considering all $2^2 \times 3^6 = 2,916$ level combinations, the experimenters adopted 18 out of them modified from an orthogonal array $OA(18, 2^1 \times 3^7)$ (see Table 5 in Joseph and Wu (2004)). In this case, for illustration purposes, we may consider a restricted design region $\mathcal{X} = [0, 160] \times \mathcal{D}$, where $[0, 160]$ is the range of the continuous factor, and $\mathcal{D} = \{(x_{i2}, \dots, x_{i9}) \mid i = 1, \dots, 18\}$ consists of the original 18 level combinations of eight discrete factors. \square

Given an experimental setting $\mathbf{x}_i = (x_{i1}, \dots, x_{id})^T \in \mathcal{X}$, suppose there are $n_i \geq 0$ experimental units assigned to this experimental setting. Their responses (could be vectors) are assumed to be iid from a parametric model $M(\mathbf{x}_i, \boldsymbol{\theta})$, where the parameter vector $\boldsymbol{\theta} \in \Theta \subseteq \mathbb{R}^p$ with the parameter space Θ . Suppose the responses are independent across different experimental settings. Under regularity conditions (see, e.g., Sections 2.5 and 2.6 in Lehmann and Casella (1998)), the corresponding Fisher information matrix can be written as $\sum_{i=1}^m n_i \mathbf{F}(\mathbf{x}_i, \boldsymbol{\theta})$, with respect to the corresponding design $\{(\mathbf{x}_i, n_i), i = 1, \dots, m\}$, known as an *exact design*, where $\mathbf{F}(\mathbf{x}_i, \boldsymbol{\theta})$ is a $p \times p$ matrix, known as the Fisher information at \mathbf{x}_i . In design theory, $\boldsymbol{\xi} = \{(\mathbf{x}_i, w_i), i = 1, \dots, m\}$ with $w_i = n_i/n \geq 0$ and $n = \sum_{i=1}^m n_i$, known as an *approximate design*, is often considered first (Kiefer, 1974; Pukelsheim, 1993; Atkinson et al., 2007). The collection of all feasible designs is denoted by $\Xi = \{(\mathbf{x}_i, w_i), i = 1, \dots, m \mid m \geq 1, \mathbf{x}_i \in \mathcal{X}, w_i \geq 0, \sum_{i=1}^m w_i = 1\}$.

2.1 EW D-optimal designs

Following Bu et al. (2020) and Huang et al. (2024), we adopt the D-criterion for optimal designs. When $\boldsymbol{\theta}$ is given or assumed to be known, an $\boldsymbol{\xi} \in \Xi$ that maximizes $f(\boldsymbol{\xi}) = |\mathbf{F}(\boldsymbol{\xi}, \boldsymbol{\theta})|$ is known as a *locally D-optimal design* (Chernoff, 1953), where $\mathbf{F}(\boldsymbol{\xi}, \boldsymbol{\theta}) = \sum_{i=1}^m w_i \mathbf{F}(\mathbf{x}_i, \boldsymbol{\theta})$ is the Fisher information matrix associated with $\boldsymbol{\xi}$. The ForLion algorithm was proposed by Huang et al. (2024) for finding locally D-optimal designs with mixed factors.

When $\boldsymbol{\theta}$ is unknown while a prior distribution or probability measure $Q(\cdot)$ on Θ is available instead, we adopt the EW D-optimality (Atkinson et al., 2007; Yang et al., 2016, 2017; Bu et al., 2020; Huang et al., 2025) and look for $\boldsymbol{\xi} \in \Xi$ maximizing

$$f_{\text{EW}}(\boldsymbol{\xi}) = |E\{\mathbf{F}(\boldsymbol{\xi}, \Theta)\}| = \left| \sum_{i=1}^m w_i E\{\mathbf{F}(\mathbf{x}_i, \Theta)\} \right|, \quad (2.1)$$

called an *integral-based EW D-optimal* approximate design, where

$$E \{ \mathbf{F}(\mathbf{x}_i, \Theta) \} = \int_{\Theta} \mathbf{F}(\mathbf{x}_i, \boldsymbol{\theta}) Q(d\boldsymbol{\theta}) \quad (2.2)$$

is a $p \times p$ matrix after entry-wise expectation with respect to $Q(\cdot)$ on Θ . By replacing $\boldsymbol{\theta}$ in $\mathbf{F}(\boldsymbol{\xi}, \boldsymbol{\theta})$ with Θ , we indicate that the expectation $E \{ \mathbf{F}(\boldsymbol{\xi}, \Theta) \}$ is taken with respect to a random parameter vector in Θ .

When $\boldsymbol{\theta}$ is unknown but a dataset from a prior or pilot study is available, following Bu et al. (2020) and Huang et al. (2025), we bootstrap the original dataset to obtain a set of bootstrapped datasets, and their corresponding parameter vectors $\{\hat{\boldsymbol{\theta}}_1, \dots, \hat{\boldsymbol{\theta}}_B\}$ obtained by fitting the parametric model on each of the bootstrapped datasets. In other words, we may replace the prior distribution $Q(\cdot)$ in (2.2) with the empirical distribution of $\{\hat{\boldsymbol{\theta}}_1, \dots, \hat{\boldsymbol{\theta}}_B\}$. That is, we may look for $\boldsymbol{\xi} \in \Xi$ maximizing

$$f_{\text{SEW}}(\boldsymbol{\xi}) = |\hat{E} \{ \mathbf{F}(\boldsymbol{\xi}, \Theta) \}| = \left| \sum_{i=1}^m w_i \hat{E} \{ \mathbf{F}(\mathbf{x}_i, \Theta) \} \right|, \quad (2.3)$$

called a *sample-based EW D-optimal* approximate design, where

$$\hat{E} \{ \mathbf{F}(\mathbf{x}_i, \Theta) \} = \frac{1}{B} \sum_{j=1}^B \mathbf{F}(\mathbf{x}_i, \hat{\boldsymbol{\theta}}_j) \quad (2.4)$$

is a bootstrapped estimate of $E \{ \mathbf{F}(\mathbf{x}_i, \Theta) \}$ based on $\{\hat{\boldsymbol{\theta}}_1, \dots, \hat{\boldsymbol{\theta}}_B\}$. According to Bu et al. (2020), the EW D-optimal design obtained via bootstrapped samples is a good approximation to the Bayesian D-optimal design obtained in a similar way.

For multinomial logistic models, such as the cumulative logit model used for the trauma clinical trial (see Example 5.2 in Bu et al. (2020)), the feasible parameter space $\Theta = \{ \boldsymbol{\theta} = (\beta_{11}, \beta_{12}, \beta_{21}, \beta_{22}, \beta_{31}, \beta_{32}, \beta_{41}, \beta_{42})^T \mid \beta_{11} + \beta_{12}x < \beta_{21} + \beta_{22}x < \beta_{31} + \beta_{32}x < \beta_{41} + \beta_{42}x, \text{ for all } x \in \mathcal{X} \}$ is not rectangular, which makes the integral in (2.2) difficult to calculate. In this case, even with a prior distribution instead of a dataset, we may also draw a random sample $\{\hat{\boldsymbol{\theta}}_1, \dots, \hat{\boldsymbol{\theta}}_B\}$ from the prior distribution, and adopt the sample-based EW D-optimality. According to Section S5 in the Supplementary Material, in terms of relative efficiency, the obtained EW D-optimal designs are fairly stable against the random samples.

2.2 Characteristics of EW D-optimal designs

Since the design region \mathcal{X} typically contains infinitely many design points, which is different in nature from the experiments considered by Yang et al. (2016, 2017) and Bu et al. (2020), both the theoretical properties and numerical algorithms for EW D-optimal designs here are far more difficult.

In this section, to characterize EW D-optimal designs, we fix either a prior distribution $Q(\cdot)$ on Θ for integral-based EW D-optimality, or a set of bootstrapped or sampled parameter vectors $\{\hat{\boldsymbol{\theta}}_1, \dots, \hat{\boldsymbol{\theta}}_B\}$ for sample-based EW D-optimality, so that either $E \{ \mathbf{F}(\mathbf{x}_i, \Theta) \}$ is defined as in (2.2), or $\hat{E} \{ \mathbf{F}(\mathbf{x}_i, \Theta) \}$ is defined as in (2.4). Similarly to

Fedorov and Leonov (2014) and Huang et al. (2024), we list the assumptions needed for this paper.

- (A1) The design region $\mathcal{X} \subset \mathbb{R}^d$ is compact.
- (A2) For each $\boldsymbol{\theta} \in \Theta$, the Fisher information $\mathbf{F}(\mathbf{x}, \boldsymbol{\theta})$ is element-wise continuous with respect to all continuous factors of $\mathbf{x} \in \mathcal{X}$.
- (A3) For each $\boldsymbol{\theta} \in \Theta$, the Fisher information $\mathbf{F}(\mathbf{x}, \boldsymbol{\theta}) = (F_{st}(\mathbf{x}, \boldsymbol{\theta}))_{s,t=1,\dots,p}$ is element-wise continuous with respect to all continuous factors of $\mathbf{x} \in \mathcal{X}$, and there exists a nonnegative and integrable function $K(\boldsymbol{\theta})$ on Θ , such that, $\int_{\Theta} K(\boldsymbol{\theta})Q(d\boldsymbol{\theta}) < \infty$, and $|F_{st}(\mathbf{x}, \boldsymbol{\theta})| \leq K(\boldsymbol{\theta})$, for all $s, t \in \{1, \dots, p\}$, $\mathbf{x} \in \mathcal{X}$, and $\boldsymbol{\theta} \in \Theta$.

In this paper, \mathcal{X} is either $\prod_{j=1}^d I_j$ or $\prod_{j=1}^k I_j \times \mathcal{D}$. Both of them are bounded and closed in \mathbb{R}^d and thus Assumption (A1) is satisfied.

As for Assumptions (A2) and (A3), (i) if $k = 0$, that is, all factors are discrete, then both Assumption (A2) and the first half (i.e., the continuous statement) of Assumption (A3) are automatically satisfied; (ii) when $k \geq 1$, that is, there is at least one continuous factor, (A3) always implies (A2).

Following Fedorov and Leonov (2014), to characterize the sample-based and integral-based D-optimal EW designs, we extend the collection Ξ of designs (each design consists only of a finite number of design points) to $\Xi(\mathcal{X})$, which consists of all probability measures on \mathcal{X} . In other words, a design $\boldsymbol{\xi} \in \Xi(\mathcal{X})$ is also a probability measure on \mathcal{X} , and for each $\boldsymbol{\theta} \in \Theta$,

$$\mathbf{F}(\boldsymbol{\xi}, \boldsymbol{\theta}) = \int_{\mathcal{X}} \mathbf{F}(\mathbf{x}, \boldsymbol{\theta})\boldsymbol{\xi}(d\mathbf{x}) .$$

Then for sample-based EW criterion and $\boldsymbol{\xi} \in \Xi(\mathcal{X})$, we denote

$$\mathbf{F}_{\text{SEW}}(\boldsymbol{\xi}) = \hat{E}\{\mathbf{F}(\boldsymbol{\xi}, \Theta)\} = \frac{1}{B} \sum_{j=1}^B \mathbf{F}(\boldsymbol{\xi}, \hat{\boldsymbol{\theta}}_j) = \int_{\mathcal{X}} \hat{E}\{\mathbf{F}(\mathbf{x}, \Theta)\}\boldsymbol{\xi}(d\mathbf{x}) . \quad (2.5)$$

For integral-based EW criterion, under Assumption (A3) and Fubini Theorem (see, for example, Theorem 5.9.2 in Resnick (2003)), we denote

$$\begin{aligned} \mathbf{F}_{\text{EW}}(\boldsymbol{\xi}) &= E\{\mathbf{F}(\boldsymbol{\xi}, \Theta)\} = \int_{\Theta} \mathbf{F}(\boldsymbol{\xi}, \boldsymbol{\theta})Q(d\boldsymbol{\theta}) \\ &= \int_{\Theta} \int_{\mathcal{X}} \mathbf{F}(\mathbf{x}, \boldsymbol{\theta})\boldsymbol{\xi}(d\mathbf{x})Q(d\boldsymbol{\theta}) \\ &= \int_{\mathcal{X}} \int_{\Theta} \mathbf{F}(\mathbf{x}, \boldsymbol{\theta})Q(d\boldsymbol{\theta})\boldsymbol{\xi}(d\mathbf{x}) \quad (\text{by Fubini Theorem}) \\ &= \int_{\mathcal{X}} E\{\mathbf{F}(\mathbf{x}, \Theta)\}\boldsymbol{\xi}(d\mathbf{x}) . \end{aligned} \quad (2.6)$$

Furthermore, we denote the collections of Fisher information matrices, $\mathcal{F}_{\text{SEW}}(\mathcal{X}) = \{\mathbf{F}_{\text{SEW}}(\boldsymbol{\xi}) \mid \boldsymbol{\xi} \in \Xi(\mathcal{X})\}$, and $\mathcal{F}_{\text{EW}}(\mathcal{X}) = \{\mathbf{F}_{\text{EW}}(\boldsymbol{\xi}) \mid \boldsymbol{\xi} \in \Xi(\mathcal{X})\}$. As a summary of the arguments in Section S2, we have the following lemma.

Lemma 1. *Under Assumptions (A1) and (A2), $\mathcal{F}_{\text{SEW}}(\mathcal{X})$ is convex and compact; while under Assumptions (A1) and (A3), $\mathcal{F}_{\text{EW}}(\mathcal{X})$ is convex and compact.*

With the aid of Lemma 1 and Carathéodory’s Theorem (see, for example, Theorem 2.1.1 in Fedorov (1972)), we obtain the following theorem, whose proof, as well as proofs for other theorems, is relegated to Section S3 in the Supplementary Material.

Theorem 1. *If Assumptions (A1) and (A2) hold, then for any $p \times p$ matrix $\mathbf{F} \in \mathcal{F}_{\text{SEW}}(\mathcal{X})$, there exists a design $\boldsymbol{\xi} \in \Xi \subset \Xi(\mathcal{X})$ with no more than $m = p(p + 1)/2 + 1$ points, such that $\mathbf{F}_{\text{SEW}}(\boldsymbol{\xi}) = \mathbf{F}$. If \mathbf{F} is a boundary point of the convex set $\mathcal{F}_{\text{SEW}}(\mathcal{X})$, then we need no more than $p(p + 1)/2$ support points for $\boldsymbol{\xi}$. If Assumptions (A1) and (A3) are satisfied, then the same conclusions hold for $\mathcal{F}_{\text{EW}}(\mathcal{X})$ and $\mathbf{F}_{\text{EW}}(\boldsymbol{\xi})$ as well.*

To characterize D-optimality for EW designs, we define the objective function $\Psi(\mathbf{F}) = -\log |\mathbf{F}|$ for $\mathbf{F} \in \mathcal{F}_{\text{SEW}}(\mathcal{X})$ or $\mathcal{F}_{\text{EW}}(\mathcal{X})$. Then $f_{\text{SEW}}(\boldsymbol{\xi}) = \exp\{-\Psi(\hat{E}\{\mathbf{F}(\boldsymbol{\xi}, \boldsymbol{\Theta})\})\}$, and $f_{\text{EW}}(\boldsymbol{\xi}) = \exp\{-\Psi(E\{\mathbf{F}(\boldsymbol{\xi}, \boldsymbol{\Theta})\})\}$. Note that minimizing $\Psi(\mathbf{F})$ for $\mathbf{F} \in \mathcal{F}_{\text{SEW}}(\mathcal{X})$ or $\mathcal{F}_{\text{EW}}(\mathcal{X})$ is equivalent to maximizing $f_{\text{SEW}}(\boldsymbol{\xi})$ or $f_{\text{EW}}(\boldsymbol{\xi})$ for $\boldsymbol{\xi} \in \Xi$, respectively, due to Theorem 1.

For D-optimality, according to Section 2.4.2 in Fedorov and Leonov (2014), Ψ always satisfies their Assumptions (B1), (B2), and (B4). In our notations, we let $\Xi(q)$ denote $\{\boldsymbol{\xi} \in \Xi \mid |\hat{E}\{\mathbf{F}(\boldsymbol{\xi}, \boldsymbol{\Theta})\}| \geq q\}$ for sample-based EW D-optimality, or $\{\boldsymbol{\xi} \in \Xi \mid |E\{\mathbf{F}(\boldsymbol{\xi}, \boldsymbol{\Theta})\}| \geq q\}$ for integral-based EW D-optimality. We still need the following assumption:

(B3) There exists a $q > 0$, such that $\Xi(q)$ is non-empty.

Theorem 2. *For sample-based EW D-optimality under Assumptions (A1), (A2), and (B3), or integral-based EW D-optimality under Assumptions (A1), (A3), and (B3), we must have (i) there exists an optimal design $\boldsymbol{\xi}^*$ that contains no more than $p(p + 1)/2$ design points; (ii) the set of optimal designs is convex; and (iii) a design $\boldsymbol{\xi}$ is EW D-optimal if and only if $\max_{\mathbf{x} \in \mathcal{X}} d(\mathbf{x}, \boldsymbol{\xi}) \leq p$, where $d(\mathbf{x}, \boldsymbol{\xi}) = \text{tr}([E\{\mathbf{F}(\boldsymbol{\xi}, \boldsymbol{\Theta})\}]^{-1}E\{\mathbf{F}(\mathbf{x}, \boldsymbol{\Theta})\})$ for integral-based EW D-optimality, or $\text{tr}([\hat{E}\{\mathbf{F}(\boldsymbol{\xi}, \boldsymbol{\Theta})\}]^{-1}\hat{E}\{\mathbf{F}(\mathbf{x}, \boldsymbol{\Theta})\})$ for sample-based EW D-optimality.*

3. Algorithms for EW D-optimal Designs

3.1 EW lift-one algorithm for discrete factors only

When all factors are discrete, the design region \mathcal{X} contains only a finite number of distinct experimental settings. In this case, we may denote the corresponding design settings as $\mathbf{x}_1, \dots, \mathbf{x}_m$. The EW D-optimal design problem in this case is to find $\mathbf{w}^* = (w_1^*, \dots, w_m^*)^T \in S = \{(w_1, \dots, w_m)^T \in \mathbb{R}^m \mid w_i \geq 0, i = 1, \dots, m; \sum_{i=1}^m w_i = 1\}$, which maximizes $f_{\text{EW}}(\mathbf{w}) = |\sum_{i=1}^m w_i E\{\mathbf{F}(\mathbf{x}_i, \boldsymbol{\Theta})\}|$ or $f_{\text{SEW}}(\mathbf{w}) = |\sum_{i=1}^m w_i \hat{E}\{\mathbf{F}(\mathbf{x}_i, \boldsymbol{\Theta})\}|$.

The lift-one algorithm (see Algorithm 3 in the Supplementary Material of Huang et al. (2025)) can be used for finding EW D-optimal designs, with $f(\mathbf{w})$ replaced by $f_{\text{EW}}(\mathbf{w})$ or $f_{\text{SEW}}(\mathbf{w})$, called *EW lift-one algorithm*.

To speed up the lift-one algorithm, Yang and Mandal (2015) provided analytic solutions in their Lemma 4.2 for generalized linear models. Bu et al. (2020) mentioned but with no details that the corresponding optimization problems for multinomial logistic models (MLM) also have analytic solutions when the number of response categories $J \leq 5$. In Section S1 of the Supplementary Material, we provide all the relevant formulae for the lift-one algorithm under an MLM with $J \leq 5$.

3.2 EW ForLion algorithm and rounding algorithm

When at least one factor is continuous, we follow the ForLion algorithm proposed by Huang et al. (2024) for locally D-optimal designs, to find EW D-optimal designs, called the *EW ForLion algorithm* (see Algorithm 1).

When there is no confusion, we denote (i) $\mathbf{F}(\boldsymbol{\xi})$ for $E\{\mathbf{F}(\boldsymbol{\xi}, \boldsymbol{\Theta})\}$ under integral-based EW D-optimality or $\hat{E}\{\mathbf{F}(\boldsymbol{\xi}, \boldsymbol{\Theta})\}$ under sample-based EW D-optimality, for each $\boldsymbol{\xi} \in \Xi$; and (ii) $\mathbf{F}_{\mathbf{x}}$ for $E\{\mathbf{F}(\mathbf{x}, \boldsymbol{\Theta})\}$ under integral-based EW D-optimality or $\hat{E}\{\mathbf{F}(\mathbf{x}, \boldsymbol{\Theta})\}$ under sample-based EW D-optimality, for each $\mathbf{x} \in \mathcal{X}$. As a result, $d(\mathbf{x}, \boldsymbol{\xi})$ in Theorem 2 can be simplified to $d(\mathbf{x}, \boldsymbol{\xi}) = \text{tr}(\mathbf{F}(\boldsymbol{\xi})^{-1}\mathbf{F}_{\mathbf{x}})$.

Algorithm 1: EW ForLion Algorithm

Step 1: Specify the merging threshold $\delta > 0$ (e.g., 10^{-2}) and the converging threshold $\epsilon > 0$ (e.g., 10^{-6}), and establish an initial design $\boldsymbol{\xi}_0 = \{(\mathbf{x}_i^{(0)}, w_i^{(0)}), i = 1, \dots, m_0\} \in \Xi$, such that, $\|\mathbf{x}_i^{(0)} - \mathbf{x}_j^{(0)}\| \geq \delta$ for all $i \neq j$, and $|\mathbf{F}(\boldsymbol{\xi}_0)| > 0$.

Step 2: Merging close design points: Given $\boldsymbol{\xi}_t = \{(\mathbf{x}_i^{(t)}, w_i^{(t)}), i = 1, \dots, m_t\} \in \Xi$ obtained at the t th iteration, detect if there are any two points $\mathbf{x}_i^{(t)}$ and $\mathbf{x}_j^{(t)}$ for which $\|\mathbf{x}_i^{(t)} - \mathbf{x}_j^{(t)}\| < \delta$. For such a pair, tentatively merge them into their midpoint $(\mathbf{x}_i^{(t)} + \mathbf{x}_j^{(t)})/2$ with combined weight $w_i^{(t)} + w_j^{(t)}$, and denote the resulting design as $\boldsymbol{\xi}_{\text{mer}}$. If $|\mathbf{F}(\boldsymbol{\xi}_{\text{mer}})| > 0$, replace the two design points with their merged one and reduce m_t by 1; otherwise, do not merge them. Stop if all such pairs have been examined.

Step 3: Given $\boldsymbol{\xi}_t \in \Xi$ after the merging step, apply the lift-one algorithm (see Algorithm 3 in the Supplementary Material of Huang et al. (2025) and Remark 1 in Huang et al. (2024)) with the convergence threshold ϵ , and obtain an EW D-optimal allocation $(w_1^*, \dots, w_{m_t}^*)^T$ for the design points $\{\mathbf{x}_1^{(t)}, \dots, \mathbf{x}_{m_t}^{(t)}\}$. Replace $w_i^{(t)}$ with w_i^* , respectively.

Step 4: Deleting step: Update $\boldsymbol{\xi}_t$ by discarding any $\mathbf{x}_i^{(t)}$ with $w_i^{(t)} = 0$.

Step 5: Adding new point: Given $\boldsymbol{\xi}_t \in \Xi$, find $\mathbf{x}^* \in \mathcal{X}$ that maximizes $d(\mathbf{x}, \boldsymbol{\xi}_t)$. More specifically, if all factors are continuous, \mathbf{x}^* can be obtained by the ‘‘L-BFGS-B’’ quasi-Newton method (Byrd et al., 1995) directly. If the first k factors are continuous with $1 \leq k \leq d - 1$, we first find

$$\mathbf{x}_{(1)}^* = \operatorname{argmax}_{\mathbf{x}_{(1)} \in \prod_{j=1}^k [a_j, b_j]} d((\mathbf{x}_{(1)}^T, \mathbf{x}_{(2)}^T)^T, \boldsymbol{\xi}_t)$$

for each $\mathbf{x}_{(2)} \in \mathcal{D} \subseteq \prod_{j=k+1}^d I_j$, and then choose $\mathbf{x}_{(2)}^*$ that yields the largest $d((\mathbf{x}_{(1)}^*)^T, \mathbf{x}_{(2)}^T, \boldsymbol{\xi}_t)$. Note that $\mathbf{x}_{(1)}^*$ depends on $\mathbf{x}_{(2)}$. Then $\mathbf{x}^* = ((\mathbf{x}_{(1)}^*)^T, (\mathbf{x}_{(2)}^*)^T)^T$.

Step 6: If $d(\mathbf{x}^*, \boldsymbol{\xi}_t) \leq p$, proceed to Step 7. Otherwise, obtain $\boldsymbol{\xi}_{t+1}$ by adding $(\mathbf{x}^*, 0)$ to $\boldsymbol{\xi}_t$ and increasing m_t by 1, and return to Step 2.

Step 7: Output $\boldsymbol{\xi}_t$ as an EW D-optimal design.

The EW ForLion algorithm is essentially applying the original ForLion algorithm proposed by Huang et al. (2024) to $\mathbf{F}(\boldsymbol{\xi})$ under an EW D-optimality. It should be noted that (i) Step 2 in Algorithm 1 is different from the merging step in the original ForLion algorithm by addressing a possible issue when the merging step leads to a degenerated $\mathbf{F}(\boldsymbol{\xi}_{\text{mer}})$, which is possible in practice; and (ii) in Step 5, a general subset \mathcal{D} is used instead of $\prod_{j=k+1}^d I_j$, which is also different from the original ForLion algorithm (see Examples 1 and 2 for motivations).

According to Step 6 in Algorithm 1, $\boldsymbol{\xi}_t$ reported by the EW ForLion algorithm satisfies $\max_{\mathbf{x} \in \mathcal{X}} d(\mathbf{x}, \boldsymbol{\xi}_t) \leq p$. As a direct conclusion of Theorem 2, we have the following corollary.

Corollary 1. *For sample-based EW D-optimality under Assumptions (A1), (A2), and (B3), or integral-based EW D-optimality under Assumptions (A1), (A3), and (B3), the design obtained by Algorithm 1 must be EW D-optimal.*

Similarly to the ForLion algorithm (Huang et al., 2024), we may relax in practice the stopping rule $d(\mathbf{x}^*, \boldsymbol{\xi}_t) \leq p$ in Step 6 to $d(\mathbf{x}^*, \boldsymbol{\xi}_t) \leq p + \epsilon$. Following the arguments in Remark 2 in Huang et al. (2024), as a direct conclusion of Theorem 2, Algorithm 1 is guaranteed to stop in finite steps.

Since the design found by Algorithm 1 is an approximate design with continuous design points, to facilitate users in practice, we propose a rounding algorithm (see Algorithm 2) to convert an approximate design to an exact design with a user-specified set of grid points. Different from the rounding algorithms proposed in the literature (see, for example, Algorithm 2 in Huang et al. (2025)), Algorithm 2 here involves rounding both the weights and the design points.

Algorithm 2: Rounding Algorithm

Step 0: Input: An approximate design $\boldsymbol{\xi} = \{(\mathbf{x}_i, w_i), i = 1, \dots, m_0\} \in \Xi$ with all $w_i > 0$ and $|\mathbf{F}(\boldsymbol{\xi})| > 0$, a pre-specified merging threshold δ_r (e.g., $\delta_r = 0.1$, typically larger than δ in Algorithm 1), grid levels (or pace lengths) L_1, \dots, L_k for the k continuous factors (e.g., $L_1 = \dots = L_k = 0.25$, typically larger than δ_r), respectively, and the total number n of experimental units.

Step 1: Merging step: For each pair of \mathbf{x}_i and \mathbf{x}_j , define their distance $d_{ij} = \|\mathbf{x}_i - \mathbf{x}_j\|$ if their levels of discrete factors are identical; and ∞ otherwise. If $d_{ij} < \delta_r$, tentatively merge \mathbf{x}_i and \mathbf{x}_j into a single design point $(w_i \mathbf{x}_i + w_j \mathbf{x}_j)/(w_i + w_j)$ with combined weight $w_i + w_j$, and denote the resulting design as $\boldsymbol{\xi}_{\text{mer}}$. If $|\mathbf{F}(\boldsymbol{\xi}_{\text{mer}})| > 0$, replace $\boldsymbol{\xi}$ with $\boldsymbol{\xi}_{\text{mer}}$; otherwise, do not merge. Stop if all such pairs have been examined.

Step 2: Rounding design points to grid levels: Round the continuous components of each design point to their nearest multiples of the corresponding L_j , $j = 1, \dots, k$.

Step 3: Allocating experimental units: First set $n_i = \lfloor nw_i \rfloor$, the largest integer no more than nw_i , and then allocate any remaining units to design points with $nw_i > n_i$, in the order of increasing $\mathbf{F}(\boldsymbol{\xi})$ the most (see Algorithm 2 in Huang et al. (2025)).

Step 4: Deleting step: Discard any \mathbf{x}_i for which $n_i = 0$.

Step 5: Output: Exact design $\{(\mathbf{x}_i, n_i), i = 1, \dots, m\}$ with $n_i > 0$ and $\sum_{i=1}^m n_i = n$.

3.3 Calculating $E\{\mathbf{F}(\mathbf{x}, \Theta)\}$ or $\hat{E}\{\mathbf{F}(\mathbf{x}, \Theta)\}$

As illustrated by Yang et al. (2016, 2017) and Bu et al. (2020), one major advantage of EW D-optimality against Bayesian D-optimality is that it optimizes $|E\{\mathbf{F}(\mathbf{x}, \Theta)\}|$ or $|\hat{E}\{\mathbf{F}(\mathbf{x}, \Theta)\}|$, instead of $E\{\log|\mathbf{F}(\mathbf{x}, \Theta)|\}$. To implement the EW ForLion algorithm (Algorithm 1) for EW D-optimal designs, in this section, we show by two examples that instead of calculating $\mathbf{F}_x = E\{\mathbf{F}(\mathbf{x}, \Theta)\}$ or $\hat{E}\{\mathbf{F}(\mathbf{x}, \Theta)\}$ directly, we may focus on key components of the Fisher information matrix to make the computation more efficiently.

Example 3. Multinomial logistic models (MLM): A general MLM (Glonck and McCullagh, 1995; Zocchi and Atkinson, 1999; Bu et al., 2020) for categorical responses with J categories can be defined by $\mathbf{C}^T \log(\mathbf{L}\boldsymbol{\pi}_i) = \boldsymbol{\eta}_i = \mathbf{X}_i\boldsymbol{\theta}$, $i = 1, \dots, m$, with $(2J - 1) \times J$ constant matrices \mathbf{C} and \mathbf{L} , category probabilities $\boldsymbol{\pi}_i = (\pi_{i1}, \dots, \pi_{iJ})^T$, $J \times p$ model matrices \mathbf{X}_i , and model parameters $\boldsymbol{\theta} \in \Theta \subseteq \mathbb{R}^p$. According to Theorem 2 of Huang et al. (2024), to calculate the Fisher information \mathbf{F}_x at $\mathbf{x} \in \mathcal{X}$, it is enough to replace u_{st}^x , or $u_{st}^x(\boldsymbol{\theta})$ as it is a function of $\boldsymbol{\theta}$, with $E\{u_{st}^x(\Theta)\} = \int_{\Theta} u_{st}^x(\boldsymbol{\theta})Q(d\boldsymbol{\theta})$ or $\hat{E}\{u_{st}^x(\Theta)\} = B^{-1} \sum_{j=1}^B u_{st}^x(\hat{\boldsymbol{\theta}}_j)$, for $s, t = 1, \dots, J$. The formulae for calculating $u_{st}^x(\boldsymbol{\theta})$ can be found in Appendix A of Huang et al. (2024). Then $\mathbf{F}(\mathbf{x}, \boldsymbol{\theta}) = \mathbf{X}_x^T \mathbf{U}_x(\boldsymbol{\theta}) \mathbf{X}_x$ according to Corollary 3.1 in Bu et al. (2020), where

$$\mathbf{X}_x = \begin{pmatrix} \mathbf{h}_1^T(\mathbf{x}) & \mathbf{0}^T & \dots & \mathbf{0}^T & \mathbf{h}_c^T(\mathbf{x}) \\ \mathbf{0}^T & \mathbf{h}_2^T(\mathbf{x}) & \ddots & \vdots & \vdots \\ \vdots & \ddots & \ddots & \mathbf{0}^T & \mathbf{h}_c^T(\mathbf{x}) \\ \mathbf{0}^T & \dots & \mathbf{0}^T & \mathbf{h}_{J-1}^T(\mathbf{x}) & \mathbf{h}_c^T(\mathbf{x}) \\ \mathbf{0}^T & \dots & \dots & \mathbf{0}^T & \mathbf{0}^T \end{pmatrix}_{J \times p} \quad (3.7)$$

with predetermined predictor functions $\mathbf{h}_j = (h_{j1}, \dots, h_{jp})^T$, $j = 1, \dots, J - 1$, $\mathbf{h}_c = (h_1, \dots, h_{pc})^T$, and $\mathbf{U}_x(\boldsymbol{\theta}) = (u_{st}^x(\boldsymbol{\theta}))_{s,t=1,\dots,J}$. Then $E\{\mathbf{F}(\mathbf{x}, \Theta)\} = \mathbf{X}_x^T E\{\mathbf{U}_x(\Theta)\} \mathbf{X}_x$ and $\hat{E}\{\mathbf{F}(\mathbf{x}, \Theta)\} = \mathbf{X}_x^T \hat{E}\{\mathbf{U}_x(\Theta)\} \mathbf{X}_x$. \square

Theorem 3. For MLMs under Assumptions (A1) and (B3), suppose all the predictor functions $\mathbf{h}_1, \dots, \mathbf{h}_{J-1}$ and \mathbf{h}_c defined in (3.7) are continuous with respect to all continuous factors of $\mathbf{x} \in \mathcal{X}$, and the parameter space $\Theta \subseteq \mathbb{R}^p$ is bounded. Then there exists an EW D-optimal design $\boldsymbol{\xi}$ that contains no more than $p(p + 1)/2$ support points, and the design obtained by Algorithm 1 must be EW D-optimal.

The boundedness of Θ in Theorem 3 is a practical requirement. For typical applications, the boundedness of a working parameter space is often needed for numerical searches for parameter estimates or theoretical derivations for desired properties (Ferguson, 1996).

Example 4. Generalized linear models (GLM): A generalized linear model (McCullagh and Nelder, 1989; Dobson and Barnett, 2018) can be defined by $E(Y_i) = \mu_i$ and

$\eta_i = g(\mu_i) = \mathbf{X}_i^T \boldsymbol{\theta}$, where g is a given link function, $\mathbf{X}_i = \mathbf{h}(\mathbf{x}_i) = (h_1(\mathbf{x}_i), \dots, h_p(\mathbf{x}_i))^T$, $i = 1, \dots, m$, and $\boldsymbol{\theta} \in \Theta \subseteq \mathbb{R}^p$ (see, for example, Section 4 in Huang et al. (2024)). Then $\mathbf{F}(\mathbf{x}, \boldsymbol{\theta}) = \nu \{\mathbf{h}(\mathbf{x})^T \boldsymbol{\theta}\} \cdot \mathbf{h}(\mathbf{x}) \mathbf{h}(\mathbf{x})^T$, where $\nu = \{(g^{-1})'\}^2 / s$ with $s(\eta_i) = \text{Var}(Y_i)$ (see Table 5 in the Supplementary Material of Huang et al. (2025) for examples of ν). To calculate $\mathbf{F}_\mathbf{x} = E\{\mathbf{F}(\mathbf{x}, \Theta)\}$ or $\hat{E}\{\mathbf{F}(\mathbf{x}, \Theta)\}$ under GLMs, it is enough to replace $\nu \{\mathbf{h}(\mathbf{x})^T \boldsymbol{\theta}\}$ with $E[\nu \{\mathbf{h}(\mathbf{x})^T \Theta\}] = \int_{\Theta} \nu \{\mathbf{h}(\mathbf{x})^T \boldsymbol{\theta}\} Q(d\boldsymbol{\theta})$ or $\hat{E}[\nu \{\mathbf{h}(\mathbf{x})^T \Theta\}] = B^{-1} \sum_{j=1}^B \nu \{\mathbf{h}(\mathbf{x})^T \hat{\boldsymbol{\theta}}_j\}$. That is, $E\{\mathbf{F}(\mathbf{x}, \Theta)\} = E[\nu \{\mathbf{h}(\mathbf{x})^T \Theta\}] \cdot \mathbf{h}(\mathbf{x}) \mathbf{h}(\mathbf{x})^T$, and $\hat{E}\{\mathbf{F}(\mathbf{x}, \Theta)\} = \hat{E}[\nu \{\mathbf{h}(\mathbf{x})^T \Theta\}] \cdot \mathbf{h}(\mathbf{x}) \mathbf{h}(\mathbf{x})^T$.

To calculate $\mathbf{F}(\boldsymbol{\xi}, \boldsymbol{\theta})$ under GLMs, instead of $\sum_{i=1}^m w_i \mathbf{F}(\mathbf{x}_i, \boldsymbol{\theta})$, we recommend its matrix form $\mathbf{F}(\boldsymbol{\xi}, \boldsymbol{\theta}) = \mathbf{X}_\xi^T \mathbf{W}_\xi(\boldsymbol{\theta}) \mathbf{X}_\xi$, where $\mathbf{X}_\xi = (\mathbf{h}(\mathbf{x}_1), \dots, \mathbf{h}(\mathbf{x}_m))^T \in \mathbb{R}^{m \times p}$, and $\mathbf{W}_\xi(\boldsymbol{\theta}) = \text{diag}\{w_1 \nu \{\mathbf{h}(\mathbf{x}_1)^T \boldsymbol{\theta}\}, \dots, w_m \nu \{\mathbf{h}(\mathbf{x}_m)^T \boldsymbol{\theta}\}\}$. Then $E\{\mathbf{F}(\boldsymbol{\xi}, \boldsymbol{\theta})\} = \mathbf{X}_\xi^T E\{\mathbf{W}_\xi(\Theta)\} \mathbf{X}_\xi$ and $\hat{E}\{\mathbf{F}(\boldsymbol{\xi}, \boldsymbol{\theta})\} = \mathbf{X}_\xi^T \hat{E}\{\mathbf{W}_\xi(\Theta)\} \mathbf{X}_\xi$. The matrix form is much more efficient when programming in R. \square

Theorem 4. *For GLMs under Assumptions (A1) and (B3), suppose all the predictor functions $\mathbf{h} = (h_1, \dots, h_p)^T$ are continuous with respect to all continuous factors of $\mathbf{x} \in \mathcal{X}$, and Θ is bounded. Then there exists an EW D-optimal design $\boldsymbol{\xi}$ that contains no more than $p(p+1)/2$ support points, and the design obtained by Algorithm 1 must be EW D-optimal.*

3.4 First-order derivative of sensitivity function

To implement the EW ForLion algorithm (Algorithm 1) for EW D-optimal designs, if there is at least one continuous factor, we need to calculate the first-order derivative of the sensitivity function $d(\mathbf{x}, \boldsymbol{\xi})$ in Theorem 2. Following the simplified notation in Section 3.2, $d(\mathbf{x}, \boldsymbol{\xi}) = \text{tr}(\mathbf{F}(\boldsymbol{\xi})^{-1} \mathbf{F}_\mathbf{x})$.

Similarly to Theorem 3 in Huang et al. (2024), we obtain the following theorem for multinomial logistic models (MLM) under EW D-optimality.

Theorem 5. *For an MLM model under Assumptions (A1) and (B3), consider $\boldsymbol{\xi} \in \Xi$ satisfying $|\mathbf{F}(\boldsymbol{\xi})| > 0$. If we denote the $p \times p$ matrix $\mathbf{F}(\boldsymbol{\xi})^{-1} = (\mathbf{E}_{st})_{s,t=1,\dots,J}$ with submatrix $\mathbf{E}_{st} \in \mathbf{R}^{p_s \times p_t}$, and $p_J = p_c$, $\mathbf{h}_j^\mathbf{x} = \mathbf{h}_j(\mathbf{x})$, $\mathbf{h}_c^\mathbf{x} = \mathbf{h}_c(\mathbf{x})$, $u_{st}^\mathbf{x} = E\{u_{st}^\mathbf{x}(\Theta)\}$ or $\hat{E}\{u_{st}^\mathbf{x}(\Theta)\}$ for simplicity, then*

$$\begin{aligned} d(\mathbf{x}, \boldsymbol{\xi}) &= \sum_{t=1}^{J-1} u_{tt}^\mathbf{x} (\mathbf{h}_t^\mathbf{x})^T \mathbf{E}_{tt} \mathbf{h}_t^\mathbf{x} + \sum_{s=1}^{J-1} \sum_{t=1}^{J-1} u_{st}^\mathbf{x} (\mathbf{h}_c^\mathbf{x})^T \mathbf{E}_{Jt} \mathbf{h}_c^\mathbf{x} \\ &+ 2 \sum_{s=1}^{J-2} \sum_{t=s+1}^{J-1} u_{st}^\mathbf{x} (\mathbf{h}_t^\mathbf{x})^T \mathbf{E}_{st} \mathbf{h}_s^\mathbf{x} + 2 \sum_{s=1}^{J-1} \sum_{t=1}^{J-1} u_{st}^\mathbf{x} (\mathbf{h}_c^\mathbf{x})^T \mathbf{E}_{sJ} \mathbf{h}_s^\mathbf{x}. \end{aligned}$$

Example 5. Multinomial logistic models (MLM): To calculate the first-order derivative of $d(\mathbf{x}, \boldsymbol{\xi})$ under MLMs, we follow Appendix C in Huang et al. (2024) after (i) $\mathbf{F}(\boldsymbol{\xi})$ is replaced with $E\{\mathbf{F}(\boldsymbol{\xi}, \Theta)\}$ or $\hat{E}\{\mathbf{F}(\boldsymbol{\xi}, \Theta)\}$; (ii) $\mathbf{F}_\mathbf{x}$ is replaced with $E\{\mathbf{F}(\mathbf{x}, \Theta)\}$ or $\hat{E}\{\mathbf{F}(\mathbf{x}, \Theta)\}$; (iii) $\mathbf{U}_\mathbf{x} = (u_{st}^\mathbf{x})_{s,t=1,\dots,J}$ with $u_{st}^\mathbf{x}$ replaced by $E\{u_{st}^\mathbf{x}(\Theta)\}$ or $\hat{E}\{u_{st}^\mathbf{x}(\Theta)\}$; and (iv) when $k \geq 1$, for $i = 1, \dots, k$, $\frac{\partial \mathbf{U}_\mathbf{x}}{\partial x_i} = (\frac{\partial u_{st}^\mathbf{x}}{\partial x_i})_{s,t=1,\dots,J}$ with $\frac{\partial u_{st}^\mathbf{x}}{\partial x_i}$ replaced by $\frac{\partial E\{u_{st}^\mathbf{x}(\Theta)\}}{\partial x_i} =$

$\frac{\partial}{\partial x_i} \int_{\Theta} u_{st}^{\mathbf{x}}(\boldsymbol{\theta}) Q(d\boldsymbol{\theta})$ or $\hat{E}\{\frac{\partial u_{st}^{\mathbf{x}}}{\partial x_i}(\boldsymbol{\Theta})\} = \frac{1}{B} \sum_{j=1}^B \frac{\partial u_{st}^{\mathbf{x}}}{\partial x_i}(\hat{\boldsymbol{\theta}}_j)$. Note that $\frac{\partial u_{st}^{\mathbf{x}}}{\partial x_i}(\hat{\boldsymbol{\theta}}_j)$ denotes $\frac{\partial u_{st}^{\mathbf{x}}}{\partial x_i}$ at $\boldsymbol{\theta} = \hat{\boldsymbol{\theta}}_j$, whose formulae can be found in Appendix C of Huang et al. (2024). \square

Example 6. Generalized linear models (GLM): Under GLMs, the sensitivity function $d(\mathbf{x}, \boldsymbol{\xi}) = E[\nu\{\mathbf{h}(\mathbf{x})^T \boldsymbol{\Theta}\}] \cdot \mathbf{h}(\mathbf{x})^T [E\{\mathbf{F}(\boldsymbol{\xi}, \boldsymbol{\Theta})\}]^{-1} \mathbf{h}(\mathbf{x})$ for $f_{\text{EW}}(\boldsymbol{\xi})$ or $\hat{E}[\nu\{\mathbf{h}(\mathbf{x})^T \boldsymbol{\Theta}\}] \cdot \mathbf{h}(\mathbf{x})^T [\hat{E}\{\mathbf{F}(\boldsymbol{\xi}, \boldsymbol{\Theta})\}]^{-1} \mathbf{h}(\mathbf{x})$ for $f_{\text{SEW}}(\boldsymbol{\xi})$. Following Section S.5 of the Supplementary Material of Huang et al. (2024), we denote $\mathbf{A}_E = [\mathbf{X}_\xi^T E\{\mathbf{W}_\xi(\boldsymbol{\Theta})\} \mathbf{X}_\xi]^{-1}$ and $\mathbf{A}_{\hat{E}} = [\mathbf{X}_\xi^T \hat{E}\{\mathbf{W}_\xi(\boldsymbol{\Theta})\} \mathbf{X}_\xi]^{-1}$. The first-order derivative of $d(\mathbf{x}, \boldsymbol{\xi})$ with respect to continuous factors $\mathbf{x}_{(1)} = (x_1, \dots, x_k)^T$ is $\frac{\partial d(\mathbf{x}, \boldsymbol{\xi})}{\partial \mathbf{x}_{(1)}} = \mathbf{h}(\mathbf{x})^T \mathbf{A}_E \mathbf{h}(\mathbf{x}) \cdot \frac{\partial E[\nu\{\mathbf{h}(\mathbf{x})^T \boldsymbol{\Theta}\}]}{\partial \mathbf{x}_{(1)}} + 2 \cdot E[\nu\{\mathbf{h}(\mathbf{x})^T \boldsymbol{\Theta}\}] \cdot \left\{ \frac{\partial \mathbf{h}(\mathbf{x})}{\partial \mathbf{x}_{(1)}^T} \right\}^T \mathbf{A}_E \mathbf{h}(\mathbf{x})$ for $f_{\text{EW}}(\boldsymbol{\xi})$, or

$$\begin{aligned} \frac{\partial d(\mathbf{x}, \boldsymbol{\xi})}{\partial \mathbf{x}_{(1)}} &= \mathbf{h}(\mathbf{x})^T \mathbf{A}_{\hat{E}} \mathbf{h}(\mathbf{x}) \cdot \left\{ \frac{\partial \mathbf{h}(\mathbf{x})}{\partial \mathbf{x}_{(1)}^T} \right\}^T \cdot \frac{1}{B} \sum_{j=1}^B \nu'\{\mathbf{h}(\mathbf{x})^T \hat{\boldsymbol{\theta}}_j\} \hat{\boldsymbol{\theta}}_j \\ &+ \frac{2}{B} \cdot \sum_{j=1}^B \nu\{\mathbf{h}(\mathbf{x})^T \hat{\boldsymbol{\theta}}_j\} \cdot \left\{ \frac{\partial \mathbf{h}(\mathbf{x})}{\partial \mathbf{x}_{(1)}^T} \right\}^T \mathbf{A}_{\hat{E}} \mathbf{h}(\mathbf{x}) \end{aligned}$$

for $f_{\text{SEW}}(\boldsymbol{\xi})$. \square

Similar to Theorem 4 in Huang et al. (2024), we obtain the following result for GLM under EW D-optimality.

Theorem 6. *For a GLM model under Assumptions (A1) and (B3), consider $\boldsymbol{\xi} \in \Xi$ satisfying $|\mathbf{X}_\xi^T \mathbf{W}_\xi \mathbf{X}_\xi| > 0$, where \mathbf{W}_ξ is either $E\{\mathbf{W}_\xi(\boldsymbol{\Theta})\}$ for integral-based EW D-optimality or $\hat{E}\{\mathbf{W}_\xi(\boldsymbol{\Theta})\}$ for sample-based EW D-optimality (see Example 4). Then $\boldsymbol{\xi}$ is EW D-optimal if and only if $\max_{\mathbf{x} \in \mathcal{X}} E[\nu\{\mathbf{h}(\mathbf{x})^T \boldsymbol{\Theta}\}] \cdot \mathbf{h}(\mathbf{x})^T [\mathbf{X}_\xi^T \mathbf{W}_\xi \mathbf{X}_\xi]^{-1} \mathbf{h}(\mathbf{x}) \leq p$ for integral-based D-optimality or $\max_{\mathbf{x} \in \mathcal{X}} \hat{E}[\nu\{\mathbf{h}(\mathbf{x})^T \boldsymbol{\Theta}\}] \cdot \mathbf{h}(\mathbf{x})^T [\mathbf{X}_\xi^T \mathbf{W}_\xi \mathbf{X}_\xi]^{-1} \mathbf{h}(\mathbf{x}) \leq p$ for sample-based EW D-optimality.*

4. Applications to Real Experiments

In this section, we use the paper feeder experiment (see Section 1 and Example 2) and a minimizing surface defects experiment (see also Example 1), both under MLMs, to illustrate the advantages gained by adopting our algorithms and the EW D-optimal designs. For examples under GLMs, please see Section S6 of the Supplementary Material.

4.1 Paper feeder experiment

In this section, we consider the motivating example mentioned in Section 1 and Example 2, the paper feeder experiment. There are eight discrete control factors and one continuous factor, the stack force, under our consideration (see Section S4 for more details). As mentioned in Section 1, instead of using two separate GLMs to model the two types of failures, `misfeed` and `multifeed`, we consider multinomial logistic models

(MLM) to model all three possible outcomes, namely `misfeed`, `normal`, and `multifeed`, at the same time. Using Akaike information criterion (AIC, Akaike (1973)) and Bayesian information criterion (BIC, Hastie et al. (2009)), we adopt a cumulative logit model with `npo` as the most appropriate model for this experiment (see Table S.1 in Section S4 of the Supplementary Material).

For this experiment, we compare ten different designs (see Tables 1 and 2): (1) “Original allocation”: the original design that collected 1,785 observations roughly uniformly at 183 distinct experimental settings; (2) “EW Bu-appro”: an approximate design obtained by applying Bu et al. (2020)’s EW lift-one algorithm on the original 183 distinct settings; (3) “EW Bu-exact”: an exact design obtained by applying Bu et al. (2020)’s EW exchange algorithm on the 183 distinct settings with $n = 1,785$; (4) “EW Bu-grid2.5” & (5) “EW Bu-grid2.5 exact”: approximate and exact designs by applying Bu et al. (2020)’s algorithms after discretizing the range $[0, 160]$ of stack force into grid points with equal space 2.5; (6) “EW ForLion”: the proposed EW D-optimal approximate design by applying Algorithm 1 to the continuous factor, stack force, ranging in $[0, 160]$; (7)~(10) exact designs obtained by applying Algorithm 2 with different grid levels or pace lengths ($L = 0.1, 0.5, 1, 2.5$) and $n = 1,785$. As mentioned in Example 2, for illustration purpose, all designs follow the same 18 runs modified from $OA(18, 2^1 \times 3^7)$ for the eight discrete factors, while their design points can be different in terms of the levels of the continuous factor. Since the feasible space of a cumulative logit model is not rectangular (see Example 5.2 in Bu et al. (2020) or Example 8 in Huang et al. (2025)), we bootstrap the original dataset to collect $B = 100$ (due to computational intensity) samples and the corresponding estimated model parameters, denoted by $\hat{\theta}_1, \hat{\theta}_2, \dots, \hat{\theta}_{100}$. All the EW designs are under the sample-based EW D-optimality with respect to the 100 parameter vectors. The constructed designs are presented in Tables S.3 and S.4 of the Supplementary Material.

In Table 1, we list the number of design points m , the computational time in seconds for obtaining the designs, the objective function values, and the relative efficiencies compared with the recommended EW ForLion design, that is, $(|\hat{E}\{\mathbf{F}(\boldsymbol{\xi}, \boldsymbol{\Theta})\}|/|\hat{E}\{\mathbf{F}(\boldsymbol{\xi}_{\text{ForLion}}, \boldsymbol{\Theta})\}|)^{1/p}$ with $p = 32$. Compared with our EW ForLion design, the original design on 183 settings only attains 63.03% relative efficiency. Having applied Bu et al. (2020)’s algorithms on the same 183 settings, the relative efficiencies of EW Bu-appro and EW Bu-exact, 88.16% and 88.15%, are not satisfactory either. When we apply Bu et al. (2020)’s algorithms on grid points with length 2.5, it takes much longer time to find EW Bu-grid2.5 and EW Bu-grid2.5 exact designs, which also need more settings (55 and 44). The EW ForLion design and its exact designs at different grid levels require the minimum number of experimental settings, less computational time, and higher relative efficiencies.

To assess the robustness of these designs, we first use the original ForLion algorithm (Huang et al., 2024) to find the corresponding locally D-optimal design $\boldsymbol{\xi}_j^*$ for each $\hat{\theta}_j$. Then the robustness of a design $\boldsymbol{\xi} \in \Xi$ can be evaluated by the 100 relative efficiencies $(|\mathbf{F}(\boldsymbol{\xi}, \hat{\theta}_j)|/|\mathbf{F}(\boldsymbol{\xi}_j^*, \hat{\theta}_j)|)^{1/p}$, $j = 1, \dots, 100$. Table 2 (see also Figure S.2 in the Supplementary Material) presents the five-number summary of the 100 relative efficiencies. Overall, the EW ForLion design is the most robust one against parameter misspecifications. For practical uses, we recommend the grid-0.1 exact design (EW ForLion exact grid0.1),

Table 1: Robust designs for the paper feeder experiment

Designs	m	Time (s)	$ \hat{E}\{\mathbf{F}(\boldsymbol{\xi}, \boldsymbol{\Theta})\} $	Relative Efficiency
Original allocation	183	-	1.342e+28	63.03%
EW Bu-appro	38	116s	6.162e+32	88.16%
EW Bu-exact	38	1095s	6.159e+32	88.15%
EW Bu-grid2.5	55	15201s	2.078e+34	98.40%
EW Bu-grid2.5 exact	44	69907s	2.078e+34	98.40%
EW ForLion	38	1853s	3.482e+34	100.00%
EW ForLion exact grid0.1	38	0.28s	2.122e+34	98.46%
EW ForLion exact grid0.5	38	0.24s	2.065e+34	98.38%
EW ForLion exact grid1	38	0.23s	1.579e+34	97.56%
EW ForLion exact grid2.5	38	0.22s	1.326e+34	97.03%

Note: Time for EW ForLion exact designs are for applying Algorithm 2 to EW ForLion (approximate) design.

which has nearly the same robustness as the EW D-optimal approximate design and the smallest number of distinct experimental settings (i.e., 38).

Table 2: Summary of 100 relative efficiencies against locally D-optimal designs for paper feeder experiment

Robust design	Min	Q_1	Median	Q_3	Max
Original allocation	0.5075	0.6005	0.6115	0.6308	0.6587
EW Bu-appro	0.6813	0.8133	0.8343	0.8488	0.8741
EW Bu-exact	0.6813	0.8134	0.8346	0.8489	0.8742
EW Bu-grid2.5	0.7592	0.9183	0.9327	0.9417	0.9513
EW Bu-grid2.5 exact	0.7594	0.9184	0.9328	0.9417	0.9515
EW ForLion	0.8363	0.9277	0.9364	0.9445	0.9542
EW ForLion exact grid0.1	0.8028	0.9276	0.9361	0.9443	0.9541
EW ForLion exact grid0.5	0.7569	0.9269	0.9363	0.9447	0.9534
EW ForLion exact grid1	0.7502	0.9163	0.9315	0.9389	0.9489
EW ForLion exact grid2.5	0.7548	0.9098	0.9253	0.9348	0.9439

4.2 Minimizing surface defects

Wu (2008) presented a study that investigated optimal parameter settings in a polysilicon deposition process for circuit manufacturing (see also Example 1). This experiment involves responses of five categories, five continuous factors, and one discrete factor (see Table S1 in the Supplementary Material of Huang et al. (2024) or Table 6 in Lukemire et al. (2022)). Lukemire et al. (2022) employed a PSO algorithm and derived a locally D-optimal approximate design with 14 support points under a cumulative logit model with p_0 , while Huang et al. (2024) applied their ForLion algorithm and obtained a locally D-optimal approximate design with 17 design points.

In practice, an experimenter may not know the precise values of some or all parameters but often has varying degrees of insight into their actual values. To construct a robust design against parameter misspecifications, we sample $B = 1000$ parameter vectors from the prior distributions listed in Table S1 of the Supplementary Material of Huang et al.

(2024) for the cumulative logit model with po as follows:

$$\log \left(\frac{\pi_{i1} + \dots + \pi_{ij}}{\pi_{i,j+1} + \dots + \pi_{iJ}} \right) = \theta_j - \beta_1 x_{i1} - \beta_2 x_{i2} - \beta_3 x_{i3} - \beta_4 x_{i4} - \beta_5 x_{i5} - \beta_6 x_{i6}$$

with $i = 1, \dots, m$, $j = 1, 2, 3, 4$, and $J = 5$, where π_{ij} is the probability that the response associated with $\mathbf{x}_i = (x_{i1}, \dots, x_{i6})^T$ falls into the j th category.

We use Algorithm 1 to construct a sample-based EW D-optimal approximate design (see the left side of Table 3). Assuming that the total number of experimental units is $n = 1000$, we apply our Algorithm 2 with $L_1 = \dots = L_5 = 1$ for continuous control variables and obtain an exact design, as shown on the right side of Table 3. Both our approximate and exact designs have 17 support points.

To compare EW ForLion D-optimal designs with Bu et al. (2020)'s EW D-optimal designs on grid points, we discretize each of the five continuous control factors into 2 or 4 evenly distributed grid points, which leads to $2 \times 2^5 = 64$ or $2 \times 4^5 = 2,048$ possible design points, respectively. Discretizations with higher number of grid points are skipped due to computational intensity. Then Bu et al. (2020)'s lift-one algorithm is applied to the discretized design region and the corresponding EW D-optimal approximate designs are constructed (EW Bu grid2 and EW Bu grid4 in Figure 1).

Table 3: EW D-optimal approximate (left) and exact (right) designs by EW ForLion and rounding algorithms for minimizing surface defects experiment

Design Point	Cleaning Method	Deposition Temp.	Deposition Pressure	Nitrogen Flow	Silane Flow	Settling Time	w_i	Design Point	Cleaning Method	Deposition Temp.	Deposition Pressure	Nitrogen Flow	Silane Flow	Settling Time	n_i
1	-1	-25.000	200.000	-150	0	0	0.0475	1	-1	-25	200	-150	0	0	48
2	1	25.000	0	0	0	0	0.0986	2	1	25	0	0	0	0	99
3	1	25.000	200.000	-150	0	16	0.0380	3	1	25	200	-150	0	16	38
4	-1	-25.000	0	0	0	16	0.1206	4	-1	-25	0	0	0	16	121
5	1	0	0	0	0	16	0.0984	5	1	0	0	0	0	16	98
6	-1	25.000	-104.910	-150	-100	16	0.0426	6	-1	25	-105	-150	-100	16	43
7	-1	14.870	-1.299	0	0	0	0.1017	7	-1	15	-1	0	0	0	102
8	1	-13.168	2.802	0	0	16	0.0399	8	1	-13	3	0	0	16	40
9	-1	25.000	111.805	0	-100	16	0.0533	9	-1	25	112	0	-100	16	53
10	-1	25.000	-72.107	0	-100	16	0.0432	10	-1	25	-72	0	-100	16	43
11	-1	-25.000	-170.690	-150	0	0	0.0401	11	-1	-25	-171	-150	0	0	40
12	1	25.000	-158.631	-150	0	16	0.0470	12	1	25	-159	-150	0	16	47
13	1	-25.000	-200.000	-150	-100	0	0.0215	13	1	-25	-200	-150	-100	0	21
14	1	-25.000	-20.500	0	-100	0	0.0843	14	1	-25	-20	0	-100	0	84
15	1	-25.000	200.000	-150	-100	0	0.0415	15	1	-25	200	-150	-100	0	42
16	1	-2.925	0.017	0	0	0	0.0294	16	1	-3	0	0	0	0	29
17	-1	-10.568	-1.093	0	0	0	0.0524	17	-1	-11	-1	0	0	0	52

To compare the robustness of different designs against parameter misspecifications, we sample 10,000 parameter vectors from the prior distribution provided in Table S1 of Huang et al. (2024). For each sampled parameter vector $\boldsymbol{\theta}_j$, we calculate the relative efficiency of a design $\boldsymbol{\xi}$ under comparison with respect to our EW ForLion approximate design $\boldsymbol{\xi}_{\text{EWForLion}}$, i.e., $(|\mathbf{F}(\boldsymbol{\xi}, \boldsymbol{\theta}_j)|/|\mathbf{F}(\boldsymbol{\xi}_{\text{EWForLion}}, \boldsymbol{\theta}_j)|)^{1/p}$ with $p = 10$ in this case.

Figure 1 shows histograms and boxplots of 10,000 relative efficiencies for Bu et al. (2020)'s EW D-optimal designs on grid-2 or grid-4 design regions, EW ForLion exact design by applying our Algorithm 2 to the EW ForLion approximate design, and locally D-optimal designs obtained by Huang et al. (2024)'s original ForLion algorithm or Lukemire et al. (2022)'s PSO. It is evident that the EW ForLion exact design performs very similar to the EW ForLion approximate design. In most cases, the original ForLion and PSO designs yield relative efficiencies less than 1. EW Bu grid4 design performs apparently better than EW Bu grid2, but not as good as EW ForLion designs. Overall we recommend our EW ForLion approximate and exact designs.

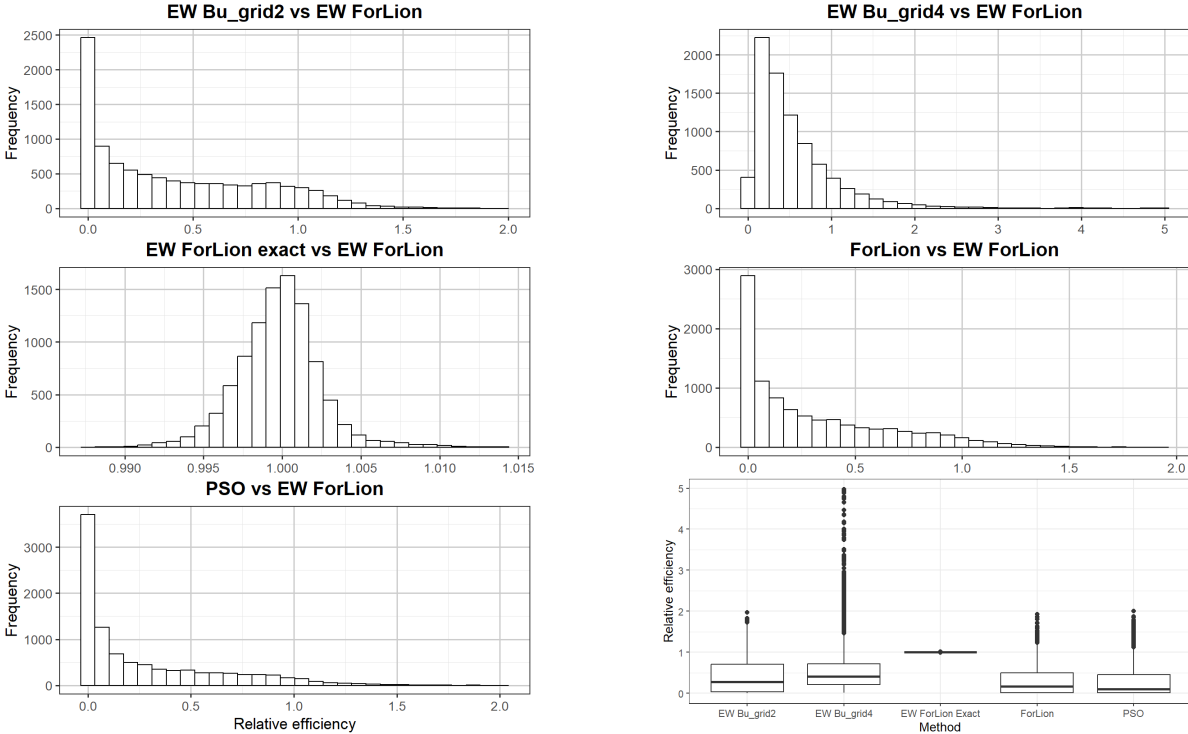


Figure 1: Relative efficiency comparison among designs for 10,000 sampled parameter sets in the minimizing surface defects experiment

5. Conclusion

In this paper, we characterize EW D-optimal designs for fairly general parametric models with mixed factors and derive detailed formulae for multinomial logistic models and generalized linear models. We develop an EW ForLion algorithm for finding EW D-optimal designs with mixed factors or continuous factors, and a rounding algorithm to convert approximate designs to exact designs.

Depending on the availability of a pilot study or a prior distribution on unknown parameters, we recommend either sample-based or integral-based EW D-optimal designs. Apparently, the obtained EW D-optimal design depends on the set of parameter vectors or the prior distribution chosen. By applying our algorithms to real experiments, we show that the obtained EW D-optimal designs under a reasonable parameter vector set or prior distribution provide well-performed robust designs against parameter misspecifications. By merging close design settings, our designs may significantly reduce the design cost and time by minimizing the number of distinct design settings.

Supplementary Materials

The Supplementary Material includes several sections: S1 provides analytic solutions for lift-one algorithm with MLMs; S2 discusses assumptions for design region and parametric models; S3 provides proofs of main theorems; S4 displays model selection and design comparison for paper feeder experiment; S5 discusses robustness of sample-based EW

designs; S6 provides two examples for GLMs and integral-based EW D-optimality.

References

- Abramowitz, M. and I. A. Stegun (1970). *Handbook of Mathematical Functions with Formulas, Graphs, and Mathematical Tables* (9th ed.). Dover Publications.
- Ai, M., Z. Ye, and J. Yu (2023). Locally d-optimal designs for hierarchical response experiments. *Statistica Sinica* 33, 381–399.
- Akaike, H. (1973). Information theory and an extension of the maximum likelihood principle. In B. Petrov and F. Csaki (Eds.), *Proceedings of the 2nd International Symposium on Information Theory*, pp. 267–281. Akademiai Kiado, Budapest.
- Atkinson, A. C., A. N. Donev, and R. D. Tobias (2007). *Optimum Experimental Designs, with SAS*. Oxford, United Kingdom: Oxford University Press.
- Billingsley, P. (1999). *Convergence of Probability Measures* (2 ed.). John Wiley & Sons.
- Bu, X., D. Majumdar, and J. Yang (2020). D-optimal designs for multinomial logistic models. *Annals of Statistics* 48(2), 983–1000.
- Byrd, R. H., P. Lu, J. Nocedal, and C. Zhu (1995). A limited memory algorithm for bound constrained optimization. *SIAM Journal on scientific computing* 16(5), 1190–1208.
- Chaloner, K. and I. Verdinelli (1995). Bayesian experimental design: a review. *Statistical Science* 10, 273–304.
- Chernoff, H. (1953). Locally optimal designs for estimating parameters. *Annals of Mathematical Statistics* 24, 586–602.
- Dobson, A. and A. Barnett (2018). *An Introduction to Generalized Linear Models* (4 ed.). Chapman & Hall/CRC.
- Fedorov, V. (1972). *Theory of Optimal Experiments*. Academic Press.
- Fedorov, V. and S. Leonov (2014). *Optimal Design for Nonlinear Response Models*. Chapman & Hall/CRC.
- Fedorov, V. V. and P. Hackl (1997). *Model-Oriented Design of Experiments*. Springer Science & Business Media.
- Ferguson, T. (1996). *A Course in Large Sample Theory*. Chapman & Hall.
- Glonek, G. and P. McCullagh (1995). Multivariate logistic models. *Journal of the Royal Statistical Society, Series B* 57, 533–546.
- Harman, R., L. Filová, and P. Richtárik (2020). A randomized exchange algorithm for computing optimal approximate designs of experiments. *Journal of the American Statistical Association* 115(529), 348–361.

- Hastie, T., R. Tibshirani, and J. Friedman (2009). *The Elements of Statistical Learning: Data Mining, Inference, and Prediction* (2 ed.). Springer.
- Huang, Y., K. Li, A. Mandal, and J. Yang (2024). Forlion: A new algorithm for d-optimal designs under general parametric statistical models with mixed factors. *Statistics and Computing* 34, 157.
- Huang, Y., L. Tong, and J. Yang (2025). Constrained d-optimal design for paid research study. *Statistica Sinica*. To appear, available at https://www3.stat.sinica.edu.tw/ss_newpaper/SS-2022-0414_na.pdf.
- Joseph, V. and C. Wu (2004). Failure amplification method: an information maximization approach to categorical response optimization (with discussions). *Technometrics* 46, 1–31.
- Kennedy, J. and R. Eberhart (1995). Particle swarm optimization. In *Proceedings of ICNN'95-International Conference on Neural Networks*, Volume 4, pp. 1942–1948. IEEE.
- Kiefer, J. (1974). General equivalence theory for optimum designs (approximate theory). *Annals of Statistics* 2, 849–879.
- Lehmann, E. L. and G. Casella (1998). *Theory of Point Estimation* (2 ed.). Springer, New York.
- Lukemire, J., A. Mandal, and W. K. Wong (2019). d-qps0: A quantum-behaved particle swarm technique for finding d-optimal designs with discrete and continuous factors and a binary response. *Technometrics* 61(1), 77–87.
- Lukemire, J., A. Mandal, and W. K. Wong (2022). Optimal experimental designs for ordinal models with mixed factors for industrial and healthcare applications. *Journal of Quality Technology* 54, 184–196.
- McCullagh, P. and J. Nelder (1989). *Generalized Linear Models* (2 ed.). Chapman and Hall/CRC.
- Phadke, M. (1989). *Quality Engineering using Robust Design*. Prentice-Hall, Englewood Cliffs.
- Poli, R., J. Kennedy, and T. Blackwell (2007). Particle swarm optimization: An overview. *Swarm Intelligence* 1, 33–57.
- Pukelsheim, F. (1993). *Optimal Design of Experiments*. John Wiley & Sons.
- Resnick, S. (2003). *A Probability Path*. Springer Science & Business Media.
- Silvey, S., D. Titterton, and B. Torsney (1978). An algorithm for optimal designs on a finite design space. *Communications in Statistics - Theory and Methods* 14, 1379–1389.

- Stufken, J. and M. Yang (2012). *Optimal designs for generalized linear models*, Chapter 4, pp. 137–164. Wiley.
- Titterton, D. (1976). Algorithms for computing d-optimal design on finite design spaces. In *Proc. of the 1976 Conf. on Information Science and Systems*, Volume 3, pp. 213–216. John Hopkins University.
- Titterton, D. (1978). Estimation of correlation coefficients by ellipsoidal trimming. *Journal of the Royal Statistical Society, Series C (Applied Statistics)* 27, 227–234.
- Tong, L., H. Volkmer, and J. Yang (2014). Analytic solutions for d-optimal factorial designs under generalized linear models. *Electronic Journal of Statistics* 8, 1322–1344.
- Wu, C. and M. Hamada (2009). *Experiments: Planning, Analysis, and Optimization* (2 ed.). Wiley.
- Wu, F.-C. (2008). Simultaneous optimization of robust design with quantitative and ordinal data. *International Journal of Industrial Engineering: Theory, Applications and Practice* 5, 231–238.
- Yang, J. and A. Mandal (2015). D-optimal factorial designs under generalized linear models. *Communications in Statistics - Simulation and Computation* 44, 2264–2277.
- Yang, J., A. Mandal, and D. Majumdar (2016). Optimal designs for 2^k factorial experiments with binary response. *Statistica Sinica* 26, 385–411.
- Yang, J., L. Tong, and A. Mandal (2017). D-optimal designs with ordered categorical data. *Statistica Sinica* 27, 1879–1902.
- Yang, M., S. Biedermann, and E. Tang (2013). On optimal designs for nonlinear models: a general and efficient algorithm. *Journal of the American Statistical Association* 108, 1411–1420.
- Yu, Y. (2010). Monotonic convergence of a general algorithm for computing optimal designs. *Annals of Statistics* 38, 1593–1606.
- Zocchi, S. and A. Atkinson (1999). Optimum experimental designs for multinomial logistic models. *Biometrics* 55, 437–444.

EW D-optimal Designs for Experiments with Mixed Factors

Siting Lin¹, Yifei Huang², and Jie Yang¹

¹University of Illinois at Chicago and ²Astellas Pharma, Inc.

Supplementary Material

- S1** Analytic Solutions for Multinomial Logistic Models
- S2** Assumptions and Relevant Results
- S3** Proofs of Main Theorems
- S4** Model Selection and Design Comparison for Paper Feeder Experiment
- S5** Robustness of Sample-based EW Designs
- S6** More Examples

S1. Analytic Solutions for Multinomial Logistic Models

According to Theorem S.9 in the Supplementary Material of Bu et al. (2020), for multinomial logistic models, given a design $\xi = \{(\mathbf{x}_i, w_i) \mid i = 1, \dots, m\} \in \Xi$, for $i \in \{1, \dots, m\}$ and $0 < z < 1$, we have

$$f_i(z) = (1-z)^{p-J+1} \sum_{j=0}^{J-1} b_j z^j (1-z)^{J-1-j},$$

$$f'_i(z) = (1-z)^{p-J} \sum_{j=1}^{J-1} b_j (j-pz) z^{j-1} (1-z)^{J-1-j} - pb_0 (1-z)^{p-1},$$

where $b_0 = f_i(0)$, $(b_{J-1}, b_{J-2}, \dots, b_1)^T = \mathbf{B}_{J-1}^{-1} \mathbf{c}$, $\mathbf{B}_{J-1} = (s^{t-1})_{s,t=1,2,\dots,J-1}$, and $\mathbf{c} = (c_1, c_2, \dots, c_{J-1})^T$ with $c_j = (j+1)^p j^{J-1-p} f_i(1/(j+1)) - j^{J-1} f_i(0)$, $j = 1, \dots, J-1$.

For typically applications, $p \geq J \geq 3$. Since $f_i(z)$ is an order- p polynomial in z with $f_i(1) = 0$, its maximum on $[0, 1]$ is attained either at $z = 0$ or at an interior point $z \in (0, 1)$ satisfying $f'_i(z) = 0$, that is,

$$\sum_{j=1}^{J-1} j b_j z^{j-1} (1-z)^{J-j-1} = p \sum_{j=0}^{J-1} b_j z^j (1-z)^{J-j-1}, \quad 0 < z < 1. \quad (\text{S1.1})$$

In Bu et al. (2020), it was mentioned that (S1.1) has analytic solutions for $J \leq 5$, while no formula was provided accordingly. In this section, we provide explicit solutions to facilitate the programming for multinomial logistic models. Note that we only need the real-valued solutions locating in $(0, 1)$ for our purposes.

According to the analytic solutions to quadratic, cubic, and quartic equations (see, for example, Sections 3.8.1~3.8.3 in Abramowitz and Stegun (1970)), we have the following results:

Lemma 2. When $J = 3$, (S1.1) can be rewritten as $A_2z^2 + A_1z + A_0 = 0$ with $A_2 = p(b_0 - b_1 + b_2)$, $A_1 = b_1(1 + p) - 2(b_0p + b_2)$, and $A_0 = b_0p - b_1$.

(i) If $A_2 = A_1 = A_0 = 0$, then (S1.1) has infinitely many solutions in $(0, 1)$ and $f_i(z) \equiv f_i(0) \geq 0$. In this case, we may choose $z = 0$ to maximize $f_i(z)$.

(ii) If $A_2 = A_1 = 0$ but $A_0 \neq 0$, then we must have $A_0 > 0$. In this case, (S1.1) has no solution, while $z = 0$ uniquely maximizes $f_i(z)$ with $z \in [0, 1]$.

(iii) If $A_2 = 0$ but $A_1 \neq 0$, then (S1.1) has a unique solution $-A_0/A_1 \in \mathbb{R}$.

(iv) If $A_2 \neq 0$ and $A_1^2 - 4A_2A_0 > 0$, then (S1.1) has two real solutions

$$\frac{-A_1 \pm \sqrt{A_1^2 - 4A_2A_0}}{2A_2}.$$

(v) If $A_2 \neq 0$ and $A_1^2 - 4A_2A_0 = 0$, then (S1.1) has only one real solution $-A_1/(2A_2)$.

(vi) If $A_2 \neq 0$ and $A_1^2 - 4A_2A_0 < 0$, then (S1.1) has no real solution.

Proof of Lemma 2: When $J = 3$, (S1.1) can be rewritten as $A_2z^2 + A_1z + A_0 = 0$ with $A_2 = p(b_0 - b_1 + b_2)$, $A_1 = b_1(1 + p) - 2(b_0p + b_2)$, $A_0 = b_0p - b_1$, and

$$f'_i(z) = -(1 - z)^{p-J}(A_2z^2 + A_1z + A_0).$$

We only need to verify case (ii). Actually, in this case, if $A_0 < 0$, then $f'_i(z) = -(1 - z)^{p-J}A_0 > 0$ for all $z \in (0, 1)$, while $f_i(0) \geq 0 = f_i(1)$ leads to a contradiction. \square

As a direct conclusion of Sections 3.8.2 in Abramowitz and Stegun (1970), we obtain the following lemma for $J = 4$:

Lemma 3. When $J = 4$, equation (S1.1) is equivalent to $A_3z^3 + A_2z^2 + A_1z + A_0 = 0$ with $A_0 = b_0p - b_1$, $A_1 = -3b_0p + b_1(2 + p) - 2b_2$, $A_2 = 3b_0p - b_1(1 + 2p) + b_2(2 + p) - 3b_3$, and $A_3 = p(-b_0 + b_1 - b_2 + b_3)$. The cases with $A_3 = 0$ has been listed in Lemma 2. If $A_3 \neq 0$, (S1.1) is equivalent to $z^3 + a_2z^2 + a_1z + a_0 = 0$ with $a_i = A_i/A_3$, $i = 0, 1, 2$. We let

$$q = \frac{a_1}{3} - \frac{a_2^2}{9}, \quad r = \frac{a_1a_2 - 3a_0}{6} - \frac{a_2^3}{27},$$

$s_1 = [r + (q^3 + r^2)^{1/2}]^{1/3}$, and $s_2 = [r - (q^3 + r^2)^{1/2}]^{1/3}$.

(i) If $q^3 + r^2 > 0$, then (S1.1) has only one real solution $s_1 + s_2 - a_2/3$.

(ii) If $q^3 + r^2 = 0$, then (S1.1) has two real solutions $z_1 = 2r^{1/3} - a_2/3$ and $z_2 = -r^{1/3} - a_2/3$.

(iii) If $q^3 + r^2 < 0$, then (S1.1) has three real solutions

$$z_1 = s_1 + s_2 - \frac{a_2}{3}, \quad z_2, z_3 = -\frac{s_1 + s_2}{2} - \frac{a_2}{3} \pm \frac{i\sqrt{3}}{2}(s_1 - s_2)$$

with $i = \sqrt{-1}$, known as the imaginary unit.

For $J = 5$, we follow the arguments for equation (12) in Tong et al. (2014)) and obtain the following results:

Lemma 4. *When $J = 5$, equation (S1.1) is equivalent to $A_4z^4 + A_3z^3 + A_2z^2 + A_1z + A_0 = 0$ with $A_0 = b_0p - b_1$, $A_1 = -4b_0p + b_1(3+p) - 2b_2$, $A_2 = 6b_0p - 3b_1(1+p) + b_2(4+p) - 3b_3$, $A_3 = -4b_0p + b_1(1+3p) - 2b_2(1+p) + b_3(3+p) - 4b_4$, and $A_4 = p(b_0 - b_1 + b_2 - b_3 + b_4)$. The cases with $A_4 = 0$ has been listed in Lemmas 3 & 2. If $A_4 \neq 0$, (S1.1) is equivalent to $z^4 + a_3z^3 + a_2z^2 + a_1z + a_0 = 0$ with $a_i = A_i/A_4$, $i = 0, 1, 2, 3$. Then there are four solutions to (S1.1) calculated as complex numbers:*

$$z_1, z_2 = -\frac{a_3}{4} - \frac{\sqrt{A_*}}{2} \pm \frac{\sqrt{B_*}}{2}, \quad z_3, z_4 = -\frac{a_3}{4} + \frac{\sqrt{A_*}}{2} \pm \frac{\sqrt{C_*}}{2}$$

with

$$\begin{aligned} A_* &= -\frac{2a_2}{3} + \frac{a_3^2}{4} + \frac{G_*}{3 \times 2^{1/3}}, \\ B_* &= -\frac{4a_2}{3} + \frac{a_3^2}{2} - \frac{G_*}{3 \times 2^{1/3}} - \frac{-8a_1 + 4a_2a_3 - a_3^3}{4\sqrt{A_*}}, \\ C_* &= -\frac{4a_2}{3} + \frac{a_3^2}{2} - \frac{G_*}{3 \times 2^{1/3}} + \frac{-8a_1 + 4a_2a_3 - a_3^3}{4\sqrt{A_*}}, \\ D_* &= \left(F_* + \sqrt{F_*^2 - 4E_*^3} \right)^{1/3}, \\ E_* &= 12a_0 + a_2^2 - 3a_1a_3, \\ F_* &= 27a_1^2 - 72a_0a_2 + 2a_2^3 - 9a_1a_2a_3 + 27a_0a_3^2, \\ G_* &= D_* + 2^{2/3}E_*/D_* . \end{aligned}$$

S2. Assumptions and Relevant Results

Following Fedorov and Leonov (2014) and Huang et al. (2024), in this section we discuss the assumptions needed for this paper in details. Note that our assumptions have been adjusted for mixed factors. Recall that a design point or experimental setting $\mathbf{x} = (x_1, \dots, x_d)^T \in \mathcal{X} \subseteq \mathbb{R}^d$. Among the $d \geq 1$ factors, the first k factors are continuous, and the last $d - k$ factors are discrete. Note that $0 \leq k \leq d$ and $k = 0$ implies no continuous factor. When $k \geq 1$, we denote $\mathbf{x}_{(1)} = (x_1, \dots, x_k)^T$ as the vector of continuous factors.

Lemma 5. *Suppose $k \geq 1$ and the parametric model $M(\mathbf{x}, \boldsymbol{\theta})$ with $\mathbf{x} \in \mathcal{X}$ and $\boldsymbol{\theta} \in \Theta$ satisfies Assumption (A2). Given $\{\hat{\boldsymbol{\theta}}_1, \dots, \hat{\boldsymbol{\theta}}_B\} \subseteq \Theta$, $\hat{E}\{\mathbf{F}(\mathbf{x}, \Theta)\} = \frac{1}{B} \sum_{j=1}^B \mathbf{F}(\mathbf{x}, \hat{\boldsymbol{\theta}}_j)$ is element-wise continuous with respect to all continuous factors of $\mathbf{x} \in \mathcal{X}$.*

The proof of Lemma 5 is straightforward. It is for sample-based EW designs. For integral-based EW designs, we need the following lemma:

Lemma 6. *Suppose $k \geq 1$ and the parametric model $M(\mathbf{x}, \boldsymbol{\theta})$ with $\mathbf{x} \in \mathcal{X}$ and $\boldsymbol{\theta} \in \Theta$ satisfies Assumption (A3). Then $E\{\mathbf{F}(\mathbf{x}, \boldsymbol{\theta})\} = \int_{\Theta} \mathbf{F}(\mathbf{x}, \boldsymbol{\theta})Q(d\boldsymbol{\theta})$ is element-wise continuous with respect to all continuous factors of $\mathbf{x} \in \mathcal{X}$.*

Proof of Lemma 6. Given any $\mathbf{x}_0 = (x_{01}, \dots, x_{0d})^T \in \mathcal{X}$, we let $\{\mathbf{x}_n = (x_{n1}, \dots, x_{nd})^T \in \mathcal{X} \mid n \geq 1\}$ be a sequence of design points, such that, $\lim_{n \rightarrow \infty} \mathbf{x}_n = \mathbf{x}_0$. If $k < d$, then we must have $(x_{n,k+1}, \dots, x_{nd}) \equiv (x_{0,k+1}, \dots, x_{0d})$ for large enough n .

For any $s, t \in \{1, \dots, p\}$, since $F_{st}(\mathbf{x}, \boldsymbol{\theta})$ is continuous with respect to $\mathbf{x}_{(1)} = (x_1, \dots, x_k)^T$, we must have $\lim_{n \rightarrow \infty} F_{st}(\mathbf{x}_n, \boldsymbol{\theta}) = F_{st}(\mathbf{x}_0, \boldsymbol{\theta})$ for each $\boldsymbol{\theta} \in \Theta$. Since (A3) is satisfied, according to the Dominated Convergence Theorem (DCT, see, for example, Theorem 5.3.3 in Resnick (2003)), we must have

$$\begin{aligned} \lim_{n \rightarrow \infty} E\{F_{st}(\mathbf{x}_n, \Theta)\} &= \lim_{n \rightarrow \infty} \int_{\Theta} F_{st}(\mathbf{x}_n, \boldsymbol{\theta}) Q(d\boldsymbol{\theta}) \\ &= \int_{\Theta} F_{st}(\mathbf{x}_0, \boldsymbol{\theta}) Q(d\boldsymbol{\theta}) \quad (\text{by DCT}) \\ &= E\{F_{st}(\mathbf{x}_0, \Theta)\} \end{aligned}$$

for each $\mathbf{x}_0 \in \mathcal{X}$, as long as $\lim_{n \rightarrow \infty} \mathbf{x}_n = \mathbf{x}_0$. That is, $E\{\mathbf{F}(\mathbf{x}, \Theta)\}$ is element-wise continuous with respect to $\mathbf{x}_{(1)}$. \square

Since the Fisher information matrices $\mathbf{F}(\mathbf{x}, \hat{\boldsymbol{\theta}}_j)$ and $\mathbf{F}(\mathbf{x}, \boldsymbol{\theta})$ are symmetric and nonnegative definite for all $\mathbf{x} \in \mathcal{X}$ and $\hat{\boldsymbol{\theta}}_j, \boldsymbol{\theta} \in \Theta$, and both integration and convex combination preserve symmetry and nonnegative definiteness, then $\mathbf{F}(\boldsymbol{\xi}, \boldsymbol{\theta})$, $\mathbf{F}(\boldsymbol{\xi}, \hat{\boldsymbol{\theta}}_j)$, $\mathbf{F}_{\text{SEW}}(\boldsymbol{\xi})$, and $\mathbf{F}_{\text{EW}}(\boldsymbol{\xi})$ are symmetric and nonnegative definite as well.

For any $\boldsymbol{\theta} \in \Theta$, $\mathbf{F}(\boldsymbol{\xi}, \boldsymbol{\theta})$ is linear in $\boldsymbol{\xi} \in \Xi(\mathcal{X})$. Actually, for any two designs $\boldsymbol{\xi}_1, \boldsymbol{\xi}_2 \in \Xi(\mathcal{X})$ and any $\lambda \in [0, 1]$, it can be verified that

$$\mathbf{F}(\lambda \boldsymbol{\xi}_1 + (1 - \lambda) \boldsymbol{\xi}_2, \boldsymbol{\theta}) = \lambda \mathbf{F}(\boldsymbol{\xi}_1, \boldsymbol{\theta}) + (1 - \lambda) \mathbf{F}(\boldsymbol{\xi}_2, \boldsymbol{\theta}) ,$$

which further implies

$$\begin{aligned} \mathbf{F}_{\text{SEW}}(\lambda \boldsymbol{\xi}_1 + (1 - \lambda) \boldsymbol{\xi}_2) &= \lambda \mathbf{F}_{\text{SEW}}(\boldsymbol{\xi}_1) + (1 - \lambda) \mathbf{F}_{\text{SEW}}(\boldsymbol{\xi}_2) , \\ \mathbf{F}_{\text{EW}}(\lambda \boldsymbol{\xi}_1 + (1 - \lambda) \boldsymbol{\xi}_2) &= \lambda \mathbf{F}_{\text{EW}}(\boldsymbol{\xi}_1) + (1 - \lambda) \mathbf{F}_{\text{EW}}(\boldsymbol{\xi}_2) . \end{aligned}$$

That is, both $\mathcal{F}_{\text{SEW}}(\mathcal{X})$ and $\mathcal{F}_{\text{EW}}(\mathcal{X})$ are convex.

Since \mathcal{X} is compact under Assumption (A1), it can be verified that $\Xi(\mathcal{X})$ is also compact under the topology of weak convergence, that is, $\boldsymbol{\xi}_n$ converges weakly to $\boldsymbol{\xi}_0$, as n goes to ∞ , if and only if $\lim_{n \rightarrow \infty} \int_{\mathcal{X}} f(\mathbf{x}) \boldsymbol{\xi}_n(d\mathbf{x}) = \int_{\mathcal{X}} f(\mathbf{x}) \boldsymbol{\xi}_0(d\mathbf{x})$ for all bounded continuous function f on \mathcal{X} (Billingsley, 1999; Fedorov and Leonov, 2014). Further with Assumption (A2), $\hat{E}\{\mathbf{F}(\mathbf{x}, \Theta)\}$ is element-wise continuous with respect to all continuous factors of $\mathbf{x} \in \mathcal{X}$ due to Lemma 5, and must be bounded due to the compactness of \mathcal{X} , then \mathbf{F}_{SEW} as a map from $\Xi(\mathcal{X})$ to $\mathbb{R}^{p \times p}$ is also bounded continuous, and thus its image $\mathcal{F}_{\text{SEW}}(\mathcal{X})$ is also compact. Similarly with Assumption (A3) and Lemma 6, \mathbf{F}_{EW} is a bounded continuous map from $\Xi(\mathcal{X})$ to $\mathbb{R}^{p \times p}$, and $\mathcal{F}_{\text{EW}}(\mathcal{X})$ is compact as well.

As a summary of the above arguments, we obtain Lemma 1.

Recall that we denote $\mathbf{F}(\boldsymbol{\xi}) = \hat{E}\{\mathbf{F}(\boldsymbol{\xi}, \Theta)\}$ for sample-based EW D-optimality, and $E\{\mathbf{F}(\boldsymbol{\xi}, \Theta)\}$ for integral-based EW D-optimality; $\mathbf{F}_{\mathbf{x}} = \hat{E}\{\mathbf{F}(\mathbf{x}, \Theta)\}$ for sample-based EW D-optimality, and $E\{\mathbf{F}(\mathbf{x}, \Theta)\}$ for integral-based EW D-optimality. Then the same set of assumptions listed in Section 2.4.2 in Fedorov and Leonov (2014) are provided in our notations as below.

(B1) $\Psi(\mathbf{F})$ is a convex function for $\mathbf{F} \in \mathcal{F}_{\text{SEW}}(\mathcal{X})$ or $\mathcal{F}_{\text{EW}}(\mathcal{X})$.

(B2) $\Psi(\mathbf{F})$ is a monotonically non-increasing function for $\mathbf{F} \in \mathcal{F}_{\text{SEW}}(\mathcal{X})$ or $\mathcal{F}_{\text{EW}}(\mathcal{X})$.

(B3) There exists a $q > 0$, such that $\Xi(q)$ is non-empty.

(B4) For any $\boldsymbol{\xi} \in \Xi(q)$, $\bar{\boldsymbol{\xi}} \in \Xi$, and $\alpha \in (0, 1)$,

$$\Psi[(1 - \alpha)\mathbf{F}(\boldsymbol{\xi}) + \alpha\mathbf{F}(\bar{\boldsymbol{\xi}})] = \Psi[\mathbf{F}(\boldsymbol{\xi})] + \alpha \int_{\mathcal{X}} \psi(\mathbf{x}, \boldsymbol{\xi}) \bar{\boldsymbol{\xi}}(d\mathbf{x}) + o(\alpha),$$

as $\alpha \rightarrow 0$, where $\psi(\mathbf{x}, \boldsymbol{\xi}) = p - \text{tr}[\mathbf{F}(\boldsymbol{\xi})^{-1}\mathbf{F}_{\mathbf{x}}]$.

According to Section 2.4.2 in Fedorov and Leonov (2014), for D-optimality, Assumptions (B1), (B2), and (B4) are always satisfied. Further discussions have been provided in Section 2.2.

S3. Proofs of Main Theorems

Proof of Theorem 1. Under Assumptions (A1) and (A2), following the proof of the lemma in Section 1.26 of Pukelsheim (1993), it can be verified that $\{\mathbf{F}_{\text{SEW}}(\boldsymbol{\xi}) \mid \boldsymbol{\xi} \in \Xi\} \subset \mathbb{R}^{p \times p}$, as the convex hull of the set $\{\hat{E}\{\mathbf{F}(\mathbf{x}, \boldsymbol{\Theta})\} \mid \mathbf{x} \in \mathcal{X}\}$ with dimension $p(p+1)/2$ due to their symmetry, is convex and compact. Due to Lemma 1 and Carathéodory's Theorem (see, for example, Theorem 2.1.1 in Fedorov (1972)), it can be further verified that for any matrix $\mathbf{F} \in \mathcal{F}_{\text{SEW}}(\mathcal{X})$ with $\boldsymbol{\xi} \in \Xi(\mathcal{X})$, there exists a $\boldsymbol{\xi}_0 \in \Xi$ with at most $p(p+1)/2+1$ design points, such that, $\mathbf{F}_{\text{SEW}}(\boldsymbol{\xi}_0) = \mathbf{F}$. When $\mathbf{F} \in \mathcal{F}_{\text{SEW}}(\mathcal{X})$ is a boundary point (that is, any open set of $\mathcal{F}_{\text{SEW}}(\mathcal{X})$ containing \mathbf{F} contains both matrices inside and outside $\mathcal{F}_{\text{SEW}}(\mathcal{X})$), the number of design points in $\boldsymbol{\xi}_0$ can be at most $p(p+1)/2$.

Similarly, we can obtain the same conclusions for $\{\mathbf{F}_{\text{EW}}(\boldsymbol{\xi}) \mid \boldsymbol{\xi} \in \Xi\}$, $\{E\{\mathbf{F}(\mathbf{x}, \boldsymbol{\Theta})\} \mid \mathbf{x} \in \mathcal{X}\}$, and $\mathcal{F}_{\text{EW}}(\mathcal{X})$ under Assumptions (A1) and (A3). \square

Proof of Theorem 2. For sample-based EW D-optimality, under Assumptions (A1), (A2), and (B3), due to Lemma 1, $\mathcal{F}_{\text{SEW}}(\mathcal{X})$ is convex and compact. Due to Assumption (B3), there exists a sample-based EW D-optimal design $\boldsymbol{\xi}_* \in \Xi(\mathcal{X})$. Due to the monotonicity of Ψ (see Assumption (B2) in Section S2), $\hat{E}\{\mathbf{F}(\boldsymbol{\xi}_*, \boldsymbol{\Theta})\}$ must be a boundary point of $\mathcal{F}_{\text{SEW}}(\mathcal{X})$. According to Theorem 1, there exists a sample-based EW D-optimal design with no more than $p(p+1)/2$ support points.

Similarly, for integral-based EW D-optimality, under Assumptions (A1), (A3), and (B3), there must exist an EW D-optimal design with no more than $p(p+1)/2$ support points.

According to Section 2.4.2 in Fedorov and Leonov (2014), Assumptions (B1), (B2), and (B4) are always satisfied for D-optimality. The rest parts of Theorem 2 are direct conclusions of Theorem 2.2 in Fedorov and Leonov (2014). \square

Proof of Theorem 3. Suppose all the predictor functions $\mathbf{h}_1, \dots, \mathbf{h}_{J-1}$ and \mathbf{h}_c defined in (3.7) are continuous with respect to all continuous factors of $\mathbf{x} \in \mathcal{X}$. Then there exists an $M_x > 0$ due to the compactness of \mathcal{X} , such that, $\|\mathbf{h}_j(\mathbf{x})\| \leq M_x$ and $\|\mathbf{h}_c(\mathbf{x})\| \leq M_x$, for all $j = 1, \dots, J-1$ and $\mathbf{x} \in \mathcal{X}$.

According to Appendix A of Huang et al. (2024), if we further have a bounded Θ , then there exists an $M_\eta > 0$, such that, $\|\boldsymbol{\eta}_{\mathbf{x}}\| = \|\mathbf{X}_{\mathbf{x}}\boldsymbol{\theta}\| \leq M_\eta$ for all $\boldsymbol{\theta} \in \Theta$ and $\mathbf{x} \in \mathcal{X}$. Then there exist $0 < \delta_x < \Delta_x < 1$, such that, $\delta_x \leq \pi_j^{\mathbf{x}}(\boldsymbol{\theta}) \leq \Delta_x$ for all $j = 1, \dots, J$, $\boldsymbol{\theta} \in \Theta$, and $\mathbf{x} \in \mathcal{X}$. Then there exists an $M_u > 0$, such that, $|u_{st}^{\mathbf{x}}(\boldsymbol{\theta})| \leq M_u$ for all $s, t = 1, \dots, J$, $\boldsymbol{\theta} \in \Theta$, and $\mathbf{x} \in \mathcal{X}$. According to Theorem 2 in Huang et al. (2024), there exists an $M_F > 0$, such that, $\|\mathbf{F}_{st}^{\mathbf{x}}(\boldsymbol{\theta})\| = \|\mathbf{F}_{st}(\mathbf{x}, \boldsymbol{\theta})\| \leq M_F$ for all $s, t = 1, \dots, J$, $\boldsymbol{\theta} \in \Theta$, and $\mathbf{x} \in \mathcal{X}$. As a direct conclusion, the Fisher information of an MLM satisfies Assumption (A3). The rest statements are direct conclusions of Theorem 2 and Corollary 1. \square

Proof of Theorem 4. Suppose all the predictor functions $\mathbf{h} = (h_1, \dots, h_p)^T$ are continuous with respect to all continuous factors of $\mathbf{x} \in \mathcal{X}$, and Θ is bounded. Since the number of level combinations of discrete factors is finite, there exist $M_x > 0$ and $M_\eta > 0$, such that, $\|\mathbf{h}(\mathbf{x})\mathbf{h}(\mathbf{x})^T\| \leq M_x$ for all $\mathbf{x} \in \mathcal{X}$, and $|\mathbf{h}(\mathbf{x})^T\boldsymbol{\theta}| \leq M_\eta$ for all $\mathbf{x} \in \mathcal{X}$ and $\boldsymbol{\theta} \in \Theta$. Since ν is continuous for commonly used GLMs (see, for example, Table 5 in the Supplementary Material of Huang et al. (2025)), there is an $M_F > 0$, such that, $|\mathbf{F}_{st}(\mathbf{x}, \boldsymbol{\theta})| \leq M_F$ for all $s, t = 1, \dots, p$, $\boldsymbol{\theta} \in \Theta$, and $\mathbf{x} \in \mathcal{X}$. As a direct conclusion, the Fisher information of a commonly used GLM satisfies Assumption (A3). The rest statements are direct conclusions of Theorem 2 and Corollary 1. \square

Proof of Theorem 5. According to Theorem 2, design $\boldsymbol{\xi}$ is EW D-optimal if and only if $\max_{\mathbf{x} \in \mathcal{X}} d(\mathbf{x}, \boldsymbol{\xi}) \leq p$. By applying Theorem 2 and its proof (see their Lemma 1) of Huang et al. (2024), we obtain

$$\text{tr}(\mathbf{E}_{st} u_{st}^{\mathbf{x}} \mathbf{h}_s^{\mathbf{x}} (\mathbf{h}_t^{\mathbf{x}})^T) = u_{st}^{\mathbf{x}} \text{tr} \left((\mathbf{h}_t^{\mathbf{x}})^T \mathbf{E}_{st} \mathbf{h}_s^{\mathbf{x}} \right) = u_{st}^{\mathbf{x}} (\mathbf{h}_t^{\mathbf{x}})^T \mathbf{E}_{st} \mathbf{h}_s^{\mathbf{x}}.$$

Note that $u_{st}^{\mathbf{x}}$ here is either $E\{u_{st}^{\mathbf{x}}(\Theta)\}$ or $\hat{E}\{u_{st}^{\mathbf{x}}(\Theta)\}$, which is different from Huang et al. (2024). \square

Proof of Theorem 6. According to Theorem 2, a necessary and sufficient condition for a design $\boldsymbol{\xi}$ to be EW D-optimal is $\max_{\mathbf{x} \in \mathcal{X}} d(\mathbf{x}, \boldsymbol{\xi}) \leq p$, which is equivalent to $\max_{\mathbf{x} \in \mathcal{X}} \text{tr}(\mathbf{F}(\boldsymbol{\xi})^{-1} \mathbf{F}_{\mathbf{x}}) \leq p$. Then the conclusions are obtained due to $\mathbf{F}(\boldsymbol{\xi}) = \mathbf{X}_{\boldsymbol{\xi}}^T \mathbf{W}_{\boldsymbol{\xi}} \mathbf{X}_{\boldsymbol{\xi}}$. \square

S4. Model Selection and Design Comparison for Paper Feeder Experiment

In this section, we provide more details about the model selection process and the designs obtained for the paper feeder experiment, which was carried out at Fuji-Xerox by Y. Norio and O. Akira (Joseph and Wu, 2004). In this experiment, there are eight discrete control factors, namely **feed belt material** (x_1 , Type A or Type B), **speed** (x_2 , 288 mm/s, 240 mm/s, or 192 mm/s), **drop height** (x_3 , 3 mm, 2 mm, or 1 mm), **center roll** (x_4 , Absent or Present), **belt width** (x_5 , 10 mm, 20 mm, or 30 mm), **tray guidance angle** (x_6 , 0, 14, or 28), **tip angle** (x_7 , 0, 3.5, or 7), and **turf** (x_8 , None, 1 sheet, or 2 sheets), one noise factor (**stack quantity**, High or Low) (see also Table 2 in Joseph and Wu (2004)), and one continuous control factor, **stack force**, taking values in $[0, 160]$ according to the original experiment. The noise factor is skipped in this analysis since it is not in control of users and is not significant either (Joseph and Wu, 2004). Following Joseph and Wu (2004), we adopt the 18 level settings of eight discrete control factors obtained by coding level 3 as level 1 in column x_4 of Table 5 in Joseph and Wu (2004).

S4.1 Model selection for paper feeder experiment

For the paper feeder experiment, the summarized response variables include the number of misfeeds y_{i1} , the number of precise feeding of the paper y_{i2} , and the number of multifeeds y_{i3} at the experimental setting \mathbf{x}_i . It is important to notice that these two types of failures, misfeed or multifeed, cannot occur simultaneously. Therefore, a multinomial logistic model is more appropriate than two separate generalized linear models for analyzing this experiment. For those three-level factors, namely x_2, x_3, x_5, x_6, x_7 , and x_8 , which are all quantitative factors, we follow Wu and Hamada (2009) and Joseph and Wu (2004) to convert the two degrees of freedom for each factor into linear and quadratic components with contrasts $(-1, 0, 1)$ and $(1, -2, 1)$, respectively. Following Joseph and Wu (2004), we code each of the two-level factors x_1 and x_4 , which are qualitative factors, as $(-1, 1)$. As for the continuous factor stack force M , we transform it to $\log(M + 1)$, which is slightly different from $\log M$ in Joseph and Wu (2004), to deal with a few cases with $M = 0$.

Table S.1: Model comparison for paper feeder experiment

	Cumulative		Continuation		Adjacent		Baseline	
	po	npo	po	npo	po	npo	po	npo
AIC	1011.06	937.87	1037.60	970.59	1027.72	962.99	1661.38	962.99
BIC	1104.34	1113.46	1130.88	1146.18	1121.00	1138.58	1754.66	1138.58

We first use AIC and BIC criteria to choose the most appropriate multinomial logistic model from eight different candidates (Bu et al., 2020). According to Table S.1, we adopt the cumulative logit model with non-proportional odds (npo), which achieves the smallest AIC and BIC values (highlighted in bold font), and is described as follows:

$$\begin{aligned}
 \log \frac{\pi_{i1}}{\pi_{i2} + \pi_{i3}} &= \beta_{11} + \beta_{12} \log(M_i + 1) + \beta_{13}x_{i1} + \beta_{14}x_{i2l} + \beta_{15}x_{i2q} \\
 &+ \beta_{16}x_{i3l} + \beta_{17}x_{i3q} + \beta_{18}x_{i4} + \beta_{19}x_{i5l} + \beta_{110}x_{i5q} + \beta_{111}x_{i6l} \\
 &+ \beta_{112}x_{i6q} + \beta_{113}x_{i7l} + \beta_{114}x_{i7q} + \beta_{115}x_{i8l} + \beta_{116}x_{i8q} , \\
 \log \frac{\pi_{i1} + \pi_{i2}}{\pi_{i3}} &= \beta_{21} + \beta_{22} \log(M_i + 1) + \beta_{23}x_{i1} + \beta_{24}x_{i2l} + \beta_{25}x_{i2q} \\
 &+ \beta_{26}x_{i3l} + \beta_{27}x_{i3q} + \beta_{28}x_{i4} + \beta_{29}x_{i5l} + \beta_{210}x_{i5q} + \beta_{211}x_{i6l} \\
 &+ \beta_{212}x_{i6q} + \beta_{213}x_{i7l} + \beta_{214}x_{i7q} + \beta_{215}x_{i8l} + \beta_{216}x_{i8q} ,
 \end{aligned}$$

where $i = 1, \dots, m$ with $m = 183$ for the original experimental design.

S4.2 Locally D-optimal designs for paper feeder experiment

Using the data listed in Table 3 of Joseph and Wu (2004), we fit the chosen model, a cumulative logit model with npo and $p = 32$ parameters. The fitted parameter values

are

$$\begin{aligned}
\hat{\boldsymbol{\theta}} &= (\hat{\beta}_{11}, \hat{\beta}_{12}, \hat{\beta}_{13}, \hat{\beta}_{14}, \hat{\beta}_{15}, \hat{\beta}_{16}, \hat{\beta}_{17}, \hat{\beta}_{18}, \\
&\hat{\beta}_{19}, \hat{\beta}_{110}, \hat{\beta}_{111}, \hat{\beta}_{112}, \hat{\beta}_{113}, \hat{\beta}_{114}, \hat{\beta}_{115}, \hat{\beta}_{116}, \\
&\hat{\beta}_{21}, \hat{\beta}_{22}, \hat{\beta}_{23}, \hat{\beta}_{24}, \hat{\beta}_{25}, \hat{\beta}_{26}, \hat{\beta}_{27}, \hat{\beta}_{28}, \\
&\hat{\beta}_{29}, \hat{\beta}_{210}, \hat{\beta}_{211}, \hat{\beta}_{212}, \hat{\beta}_{213}, \hat{\beta}_{214}, \hat{\beta}_{215}, \hat{\beta}_{216})^T \\
&= (7.995, -3.268, -1.275, 1.531, 0.044, -0.156, -0.141, 0.534, \\
&-0.261, 0.418, -1.749, -0.084, -0.207, 0.759, 0.782, 0.356, \\
&10.928, -2.461, -0.409, 0.711, 0.080, -0.144, -0.120, 0.196, \\
&0.019, -0.023, -0.931, -0.012, -0.133, 0.153, 0.128, 0.125)^T .
\end{aligned}$$

Assuming $\hat{\boldsymbol{\theta}}$ to be the true values of the model parameters, we first apply the ForLion algorithm proposed by Huang et al. (2024) and obtain a locally D-optimal approximate design, which consists of 41 design points and is listed as “ForLion” in both Table S.2 and Table S.4. To convert this approximate design with a continuous factor to an exact design, we apply our rounding algorithm (Algorithm 2) to it with merging threshold $\delta_r = 3.2$, grid level $L = 2.5$, and the number of experimental units $n = 1,785$ (the same sample size as in the original experiment). The obtained exact design is listed as “ForLion exact grid2.5” in Tables S.2 and S.4. For comparison purpose, we also apply the lift-one and exchange algorithms of Bu et al. (2020) to two different sets of design points: one set is the same as the original experiment, and the other is based on the grid points of stack force with pace length 2.5 (that is, $\{0, 2.5, 5, \dots, 157.5, 160\}$) for each of the 18 experimental settings (runs) of the eight discrete factors. The designs obtained correspondingly are presented as “Bu-appro” (lift-one algorithm on original design points) and “Bu-exact” (exchange algorithm on original design points) in Tables S.2 and S.3, and “Bu-grid2.5” (lift-one algorithm on grid-2.5 points) and “Bu-grid2.5 exact” (exchange algorithm on grid-2.5 points) in Tables S.2 and S.4. According to the summarized information of those designs listed in Table S.2, the ForLion design and its exact designs obtained by Algorithm 2 with grid level $L = 0.1, 0.5, 1, 2.5$, respectively, achieve the highest relative efficiencies with respect to the ForLion design itself, as well as the fewest design points. On the contrary, the lift-one and exchange algorithms of Bu et al. (2020) are much more time-consuming even with grid level 2.5, and the original design and Bu’s designs (Bu-appro and Bu-exact) on the original set of design points are not satisfactory in terms of relative efficiency.

The ForLion exact designs (with grid-0.1, grid-0.5, grid-1, and grid-2.5) in Table S.2 also show the convenience by adopting our rounding algorithm (Algorithm 2). Once an optimal approximate design is obtained, the exact design with a user-specified grid level can be obtained instantly with high relative efficiency. To show how we choose the merging threshold $\delta_r = 3.2$ for this experiment, in Figure S.1 we show how the relative efficiency (left panel) and the number of design points (right panel) change along with the relative distance (i.e., the merging threshold δ_r), where the grid levels 0.1, 0.5, 1 and 2.5, and the relative distances between 2 and 6 with increment of 0.1 are used for illustration. Notably, the next change on the number of design points after $\delta_r = 3.2$ will not occur until $\delta_r = 31.29$, which is too large. As a result, we recommend the merging threshold $\delta_r = 3.2$ for this experiment. The choice of grid level typically depends control accuracy of the factors and the options that the experimenter may have. As illustrated in Table S.2, the experimenter may choose the smallest possible grid level when applicable.

Table S.2: Locally D-optimal designs for paper feeder experiment

Designs	m	Time (s)	$ \mathbf{F}(\boldsymbol{\xi}, \boldsymbol{\theta}) $	Relative Efficiency
Original allocation	183	-	1.164e+28	62.792%
Bu-appro	41	62.58s	5.930e+32	88.106%
Bu-exact	41	1598s	5.928e+32	88.105%
Bu-grid2.5 appro	50	81393s	2.397e+34	98.903%
Bu-grid2.5 exact	48	85443s	2.396e+34	98.902%
ForLion	41	22099s	3.411e+34	100.000%
ForLion exact grid-0.1	36	0.01s	3.412e+34	100.001%
ForLion exact grid-0.5	36	0.01s	3.374e+34	99.965%
ForLion exact grid-1	36	0.01s	2.556e+34	99.102%
ForLion exact grid-2.5	36	0.01s	2.245e+34	98.701%

Note: m is the number of design points; Relative Efficiency is $(|\mathbf{F}(\boldsymbol{\xi}, \hat{\boldsymbol{\theta}})|/|\mathbf{F}(\boldsymbol{\xi}_{\text{ForLion}}, \hat{\boldsymbol{\theta}})|)^{1/p}$ with $p = 32$.

S4.3 More graphs and tables for paper feeder experiment

In this section, we provide *(i)* Figure S.2 for boxplots of relative efficiencies of different robust designs with respect to locally D-optimal designs, which is a graphical display of Table 2; *(ii)* Table S.3 for listing designs constructed on the set of design points of the original experiment, including Original (design), Bu-exact by Bu et al. (2020)'s exchange algorithm, Bu-appro by Bu et al. (2020)'s lift-one algorithm, EW Bu-exact by Bu et al. (2020)'s EW exchange algorithm, and EW Bu-appro by Bu et al. (2020)'s EW lift-one algorithm; and *(iii)* Table S.4 for listing designs constructed on grid points of $[0, 160]$ for stack force.

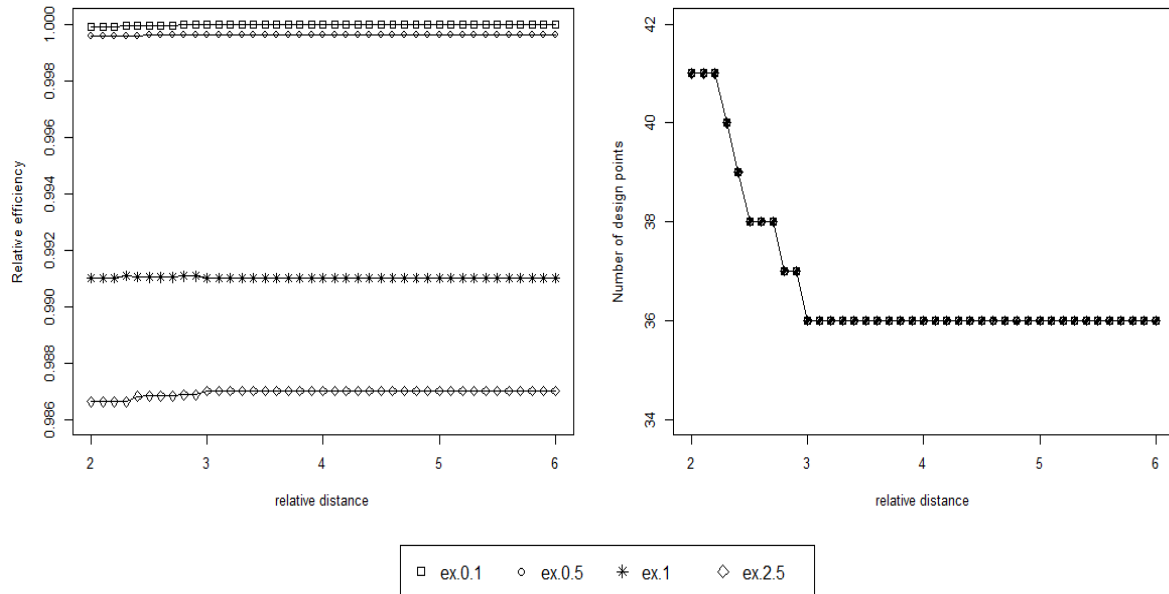


Figure S.1: Relative efficiency and number of design points of exact designs against relative distance (or merging threshold) for paper feeder experiment

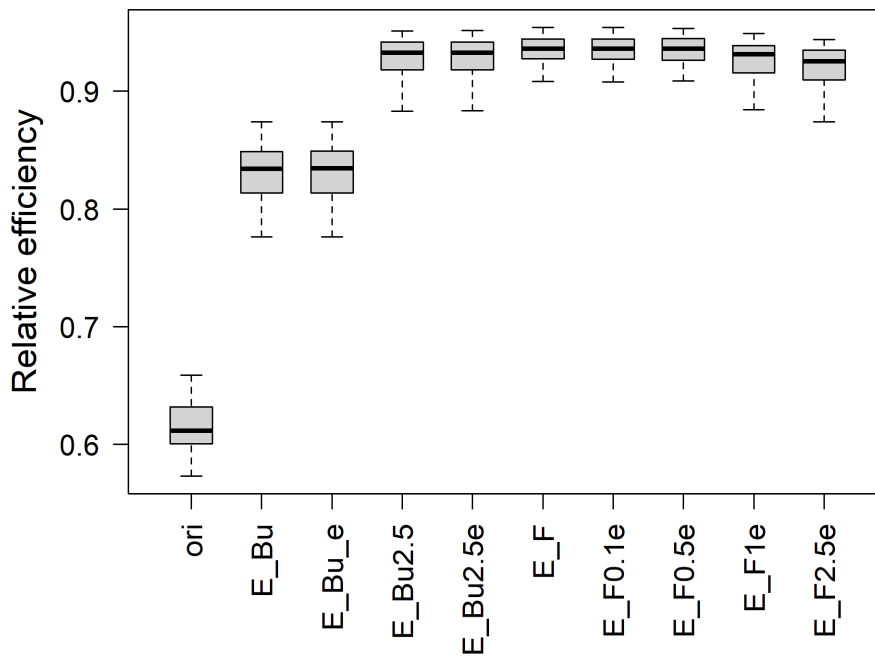


Figure S.2: Boxplots of relative efficiencies of designs in Table 2 with respect to locally D-optimal designs under 100 different sets of parameter values for paper feeder experiment

Table S.3: Designs constructed on the original set of design points for paper feeder experiment

Run	Design	Stack Force																												
		0	5	10	15	20	25	30	35	40	42.5	45	50	55	60	62.5	65	70	75	80	82.5	85	90	95	100	105	110	120	160	
1	Original					10		5		10	5	5	10		15	5	5	10		10	5	5	10					5	5	
	Bu-exact					59		0		0	0	0	0		0	0	0	0		0	0	0	0					50	0	
	Bu-appro					0.033		0		0	0	0	0		0	0	0	0		0	0	0	0					0.028	0	
	EW Bu-exact					57		0		0	0	0	0		0	0	0	0		0	0	0	0					48	0	
EW Bu-appro					0.032		0		0	0	0	0		0	0	0	0		0	0	0	0					0.027	0		
2	Original	10		10	10	10		15	5	20			5	15			5	5	5											
	Bu-exact	0		54	0	0		0	0	0			0	0			0	0	50											
	Bu-appro	0		0.030	0	0		0	0	0			0	0			0	0	0.028											
	EW Bu-exact	0		53	0	0		0	0	0			0	0			0	0	50											
EW Bu-appro	0		0.029	0	0		0	0	0			0	0			0	0	0.028												
3	Original	15		10	10	20	10	15	5	15																				
	Bu-exact	0		57	0	0		0	0	0																				
	Bu-appro	0		0.032	0	0		0	0	0																				
	EW Bu-exact	0		56	0	0		0	0	0																				
EW Bu-appro	0		0.031	0	0		0	0	0																					
4	Original	5				10	10	10		15			10	5	15			5	5	5										
	Bu-exact	0				53	0	0		0			0	0	0			0	0	48										
	Bu-appro	0				0.030	0	0		0			0	0	0			0	0	0.027										
	EW Bu-exact	42				49	0	0		0			0	0	0			0	0	47										
EW Bu-appro	0.024				0.028	0	0		0			0	0	0			0	0	0.026											
5	Original					10	10	15		20			5	20	5	10														
	Bu-exact					58	0	0		0			0	0	0	48														
	Bu-appro					0.033	0	0		0			0	0	0	0.027														
	EW Bu-exact					58	0	0		0			0	0	0	47														
EW Bu-appro					0.032	0	0		0			0	0	0	0.026															
6	Original				10	10		15		20			5	10	5	5														
	Bu-exact				55	0		0		0			0	0	0	44														
	Bu-appro				0.031	0		0		0			0	0	0	0.025														
	EW Bu-exact				53	0		0		0			0	0	0	43														
EW Bu-appro				0.030	0		0		0			0	0	0	0.024															
7	Original			10		20	5	20	10	20			5		5			5		5										
	Bu-exact			0		59	0	0	0	0			0	0	0			0		52										
	Bu-appro			0		0.033	0	0	0	0			0	0	0			0		0.029										
	EW Bu-exact			0		57	0	0	0	0			0	0	0			0		50										
EW Bu-appro			0		0.032	0	0	0	0			0	0	0			0		0.028											
8	Original				5	10		10	10	10					10			15	5	10							10		5	5
	Bu-exact				0	0		14	39	0					0			0	0	0						0		0	46	0
	Bu-appro				0	0		0.008	0.022	0					0			0	0	0						0		0	0.026	0
	EW Bu-exact				0	0		0	52	0					0			0	0	0						0		0	43	0
EW Bu-appro				0	0		0	0.029	0					0			0	0	0						0		0	0.024	0	
9	Original			10	10	10	5	10		20			5	5	10			5	10	5										
	Bu-exact			0	0	2	53	0		0			0	0	0			0	0	48										
	Bu-appro			0	0	0.001	0.029	0		0			0	0	0			0	0	0.027										
	EW Bu-exact			0	0	0	53	0		0			0	0	0			0	0	46										
EW Bu-appro			0	0	0	0.030	0		0			0	0	0			0	0	0.026											
10	Original	15		20	15	20		20		10																				
	Bu-exact	0		21	0	0		0		44																				
	Bu-appro	0		0.012	0	0		0		0.025																				
	EW Bu-exact	0		22	0	0		0		44																				
EW Bu-appro	0		0.013	0	0		0		0.025																					
11	Original	15		20	20	20		10																						
	Bu-exact	0		32	0	0		0		44																				
	Bu-appro	0		0.018	0	0		0		0.024																				
	EW Bu-exact	0		30	0	0		0		44																				
EW Bu-appro	0		0.017	0	0		0		0.024																					
12	Original	10		10	10	10		5		10			5	10	5	5														
	Bu-exact	0		26	33	0		0		0			0	0	0	51														
	Bu-appro	0		0.015	0.018	0		0		0			0	0	0	0.029														
	EW Bu-exact	0		27	30	0		0		0			0	0	0	50														
EW Bu-appro	0		0.015	0.017	0		0		0			0	0	0	0.028															
13	Original	10		10	10	10		5		5			5	5					5		5	5					5			
	Bu-exact	0		0	58	0		0		0			0	0	0			0		0		0	0			0		0	50	0
	Bu-appro	0		0	0.032	0		0		0			0	0	0			0		0		0	0			0.028				
	EW Bu-exact	0		0	56	0		0		0			0	0	0			0		0		0	0			0		0	50	0
EW Bu-appro	0		0	0.031	0		0		0			0	0	0			0		0		0	0			0.028					
14	Original			10		20	15	20	20	20			5	5																

Continued on next page

Run	Design	Stack Force																											
		0	5	10	15	20	25	30	35	40	42.5	45	50	55	60	62.5	65	70	75	80	82.5	85	90	95	100	105	110	120	160
	Bu-exact			3		52	0	0	0	0		0	43																
	Bu-appro			0.002		0.029	0	0	0	0		0	0.024																
	EW Bu-exact			0		53	0	0	0	0		0	42																
	EW Bu-appro			0		0.029	0	0	0	0		0	0.024																
15	Original	10	10	15	15	15		10	5	5		5																	
	Bu-exact	47	0	0	0	0		0	46	0		0																	
	Bu-appro	0.026	0	0	0	0		0	0.026	0		0																	
	EW Bu-exact	46	0	0	0	0		0	46	0		0																	
	EW Bu-appro	0.026	0	0	0	0		0	0.026	0		0																	
16	Original		10	10		15		20	10	15		10	5	10															
	Bu-exact		49	0		0		0	0	0		0	0	45															
	Bu-appro		0.028	0		0		0	0	0		0	0	0.025															
	EW Bu-exact		49	0		0		0	0	0		0	0	45															
	EW Bu-appro		0.027	0		0		0	0	0		0	0	0.025															
17	Original		10		10	5		10		10		5	5							5		5	5	10	5	5			
	Bu-exact		0		51	0		0		0		0	0							0		0	0	0	0	47			
	Bu-appro		0		0.029	0		0		0		0	0							0		0	0	0	0	0.027			
	EW Bu-exact		0		51	0		0		0		0	0							0		0	0	0	0	46			
	EW Bu-appro		0		0.028	0		0		0		0	0							0		0	0	0	0	0.026			
18	Original		10		5	10		10	5	5				10		5	10	5	10					10				5	
	Bu-exact		0		6	53		0	0	0		0	0	0		0	0	0	0				51				0		
	Bu-appro		0		0.003	0.030		0	0	0		0	0	0		0	0	0	0				0.029				0		
	EW Bu-exact		0		0	57		0	0	0		0	0	0		0	0	0	0				50				0		
	EW Bu-appro		0		0	0.032		0	0	0		0	0	0		0	0	0	0				0.028				0		

Table S.4: Designs on $[0, 160]$ of stack force for paper feeder experiment

Run	Design	Stack Force				w_i or n_i			
1	Bu-grid2.5	20.0	112.5	-	-	0.0305	0.0264	-	-
	Bu-grid2.5 exact	20.0	112.5	-	-	55	47	-	-
	ForLion	21.839	110.554	-	-	0.0292	0.0270	-	-
	ForLion exact grid2.5	22.5	110.0	-	-	52	48	-	-
	EW Bu-grid2.5	20.0	22.5	110	112.5	0.0173	0.0124	0.0065	0.0189
	EW Bu-grid2.5 exact	20.0	22.5	112.5	-	30	23	45	-
	EW ForLion	22.127	111.339	-	-	0.0288	0.0255	-	-
EW ForLion exact grid2.5	22.5	112.5	-	-	51	45	-	-	
2	Bu-grid2.5	5.0	75.0	-	-	0.0291	0.0279	-	-
	Bu-grid2.5 exact	5.0	75.0	-	-	52	50	-	-
	ForLion	4.749	74.807	-	-	0.0286	0.0280	-	-
	ForLion exact grid2.5	5.0	75.0	-	-	51	50	-	-
	EW Bu-grid2.5	5.0	75.0	77.5	-	0.0284	0.0169	0.0110	-
	EW Bu-grid2.5 exact	5.0	75.0	77.5	-	51	37	13	-
	EW ForLion	4.505	75.677	-	-	0.0281	0.0280	-	-
EW ForLion exact grid2.5	5.0	75.0	-	-	50	50	-	-	
3	Bu-grid2.5	7.5	47.5	-	-	0.0284	0.0257	-	-
	Bu-grid2.5 exact	7.5	47.5	-	-	51	46	-	-
	ForLion	7.669	46.322	-	-	0.0284	0.0261	-	-
	ForLion exact grid2.5	7.5	47.5	-	-	51	47	-	-
	EW Bu-grid2.5	7.5	45.0	47.5	-	0.0279	0.0055	0.0197	-
	EW Bu-grid2.5 exact	7.5	45.0	47.5	-	50	4	41	-
	EW ForLion	7.735	46.387	-	-	0.0279	0.0252	-	-
EW ForLion exact grid2.5	7.5	47.5	-	-	50	45	-	-	
4	Bu-grid2.5	17.5	20.0	97.5	100	0.0055	0.0237	0.0175	0.0084
	Bu-grid2.5 exact	17.5	20.0	97.5	100	10	42	34	12
	ForLion	18.476	97.700	-	-	0.0288	0.0268	-	-
	ForLion exact grid2.5	17.5	97.5	-	-	51	48	-	-
	EW Bu-grid2.5	0.0	20.0	100.0	102.5	0.0253	0.0270	0.0114	0.0136
	EW Bu-grid2.5 exact	0.0	20.0	100.0	102.5	45	48	5	40
	EW ForLion	0.000	19.984	100.379	-	0.0190	0.0265	0.0242	-
EW ForLion exact grid2.5	0.0	20.0	100.0	-	34	47	43	-	
5	Bu-grid2.5	15.0	82.5	-	-	0.0321	0.0287	-	-
	Bu-grid2.5 exact	15.0	82.5	-	-	57	51	-	-
	ForLion	13.925	83.114	-	-	0.0315	0.0294	-	-
	ForLion exact grid2.5	15.0	82.5	-	-	56	53	-	-
	EW Bu-grid2.5	15.0	82.5	85.0	-	0.0314	0.0245	0.0033	-
	EW Bu-grid2.5 exact	15.0	82.5	-	-	56	50	-	-
	EW ForLion	14.527	83.063	-	-	0.0311	0.0280	-	-
EW ForLion exact grid2.5	15.0	82.5	-	-	55	50	-	-	
6	Bu-grid2.5	12.5	15.0	87.5	-	0.0075	0.0229	0.0251	-
	Bu-grid2.5 exact	12.5	15.0	87.5	-	14	40	45	-
	ForLion	12.212	86.679	-	-	0.0277	0.0259	-	-
	ForLion exact grid2.5	12.5	87.5	-	-	49	46	-	-
	EW Bu-grid2.5	12.5	15.0	85.0	87.5	0.0239	0.0047	0.0046	0.0203
	EW Bu-grid2.5 exact	12.5	15.0	87.5	-	43	8	45	-
	EW ForLion	12.682	87.709	-	-	0.0273	0.0250	-	-
EW ForLion exact grid2.5	12.5	87.5	-	-	49	45	-	-	
7	Bu-grid2.5	20.0	92.5	-	-	0.0329	0.0290	-	-
	Bu-grid2.5 exact	20.0	92.5	-	-	59	52	-	-
	ForLion	18.005	20.767	90.517	-	0.0048	0.0282	0.0299	-
	ForLion exact grid2.5	20.0	90.0	-	-	59	53	-	-
	EW Bu-grid2.5	20.0	90.0	92.5	95.0	0.0322	0.0001	0.0254	0.0023
	EW Bu-grid2.5 exact	20.0	92.5	-	-	57	50	-	-
	EW ForLion	20.206	92.451	-	-	0.0323	0.0277	-	-
EW ForLion exact grid2.5	20.0	92.5	-	-	58	49	-	-	
8	Bu-grid2.5	35.0	160	-	-	0.0275	0.0261	-	-
	Bu-grid2.5 exact	35.0	160	-	-	49	47	-	-
	ForLion	33.541	35.854	160	-	0.0224	0.0048	0.0268	-
	ForLion exact grid2.5	35.0	160	-	-	49	48	-	-
	EW Bu-grid2.5	35.0	160.0	-	-	0.0272	0.0251	-	-
	EW Bu-grid2.5 exact	35.0	160.0	-	-	49	45	-	-
	EW ForLion	33.863	160	-	-	0.0269	0.0252	-	-
EW ForLion exact grid2.5	35.0	160	-	-	48	45	-	-	
9	Bu-grid2.5	22.5	25.0	110.0	-	0.0111	0.0199	0.0265	-
	Bu-grid2.5 exact	22.5	25.0	110.0	-	19	36	47	-
	ForLion	24.964	27.906	106.844	-	0.0227	0.0075	0.0275	-
	ForLion exact grid2.5	25.0	107.5	-	-	54	49	-	-
	EW Bu-grid2.5	25.0	112.5	115.0	-	0.0302	0.0160	0.0090	-
	EW Bu-grid2.5 exact	25.0	112.5	-	-	54	45	-	-
	EW ForLion	1.398	26.346	115.877	-	0.0127	0.0275	0.0235	-
EW ForLion exact grid2.5	2.5	27.5	115.0	-	23	49	42	-	
10	Bu-grid2.5	2.5	45.0	-	-	0.0253	0.0247	-	-
	Bu-grid2.5 exact	2.5	45.0	-	-	45	44	-	-
	ForLion	1.573	44.645	-	-	0.0249	0.0247	-	-
	ForLion exact grid2.5	2.5	45.0	-	-	45	44	-	-
	EW Bu-grid2.5	2.5	45.0	-	-	0.0245	0.0247	-	-
	EW Bu-grid2.5 exact	2.5	45.0	-	-	44	44	-	-
	EW ForLion	1.588	44.899	-	-	0.0247	0.0248	-	-
EW ForLion exact grid2.5	2.5	45.0	-	-	44	44	-	-	
11	Bu-grid2.5	2.5	32.5	35.0	-	0.0254	0.0208	0.0038	-
	Bu-grid2.5 exact	2.5	32.5	35.0	-	45	38	6	-
	ForLion	2.105	33.392	-	-	0.0254	0.0247	-	-
	ForLion exact grid2.5	2.5	32.5	-	-	46	44	-	-
	EW Bu-grid2.5	2.5	32.5	-	-	0.0248	0.0245	-	-
	EW Bu-grid2.5 exact	2.5	32.5	-	-	44	44	-	-
	EW ForLion	1.913	33.162	-	-	0.0250	0.0247	-	-
EW ForLion exact grid2.5	2.5	32.5	-	-	45	44	-	-	
12	Bu-grid2.5	12.5	15.0	95.0	97.5	0.0302	0.0004	0.0042	0.0241
	Bu-grid2.5 exact	12.5	15.0	95.0	97.5	54	1	5	46
	ForLion	12.553	96.478	-	-	0.0304	0.0284	-	-
	ForLion exact grid2.5	12.5	97.5	-	-	54	51	-	-
	EW Bu-grid2.5	12.5	92.5	95.0	-	0.0303	0.0120	0.0158	-
	EW Bu-grid2.5 exact	12.5	92.5	95.0	-	54	25	-	-
	EW ForLion	12.194	94.016	-	-	0.0301	0.0279	-	-
EW ForLion exact grid2.5	12.5	95.0	-	-	54	50	-	-	
13	Bu-grid2.5	12.5	15.0	92.5	95.0	0.0187	0.0130	0.0224	0.0061
	Bu-grid2.5 exact	12.5	15.0	92.5	95.0	33	24	41	10
	ForLion	14.693	92.175	-	-	0.0312	0.0287	-	-
	ForLion exact grid2.5	15.0	92.5	-	-	56	51	-	-
	EW Bu-grid2.5	12.5	15.0	92.5	95.0	0.0034	0.0276	0.0098	0.0179
	EW Bu-grid2.5 exact	12.5	15.0	95	-	54	49	-	-
	EW ForLion	14.488	93.508	-	-	0.0306	0.0279	-	-

Continued on next page

Continued

Run	Design	Stack Force				w_i or n_i			
	EW ForLion exact grid2.5	15.0	92.5	-	-	55	50	-	-
14	Bu-grid2.5	15.0	17.5	77.5	80.0	0.0082	0.0217	0.0025	0.0235
	Bu-grid2.5 exact	15.0	17.5	80	-	14	39	46	-
	ForLion	16.439	18.660	76.924	-	0.0207	0.0090	0.0269	-
	ForLion exact grid2.5	17.5	77.5	-	-	53	48	-	-
	EW Bu-grid2.5	17.5	80.0	82.5	-	0.0291	0.0192	0.0056	-
	EW Bu-grid2.5 exact	17.5	80.0	-	-	52	44	-	-
	EW ForLion	17.449	80.152	-	-	0.0291	0.0249	-	-
	EW ForLion exact grid2.5	17.5	80.0	-	-	52	44	-	-
15	Bu-grid2.5	0.0	32.5	-	-	0.0242	0.0247	-	-
	Bu-grid2.5 exact	0.0	32.5	-	-	43	44	-	-
	ForLion	0.462	32.783	-	-	0.0247	0.0246	-	-
	ForLion exact grid2.5	0.0	32.5	-	-	44	44	-	-
	EW Bu-grid2.5	0.0	32.5	-	-	0.0226	0.0248	-	-
	EW Bu-grid2.5 exact	0.0	32.5	-	-	40	44	-	-
	EW ForLion	0.483	32.917	-	-	0.0245	0.0248	-	-
	EW ForLion exact grid2.5	0.0	32.5	-	-	44	44	-	-
16	Bu-grid2.5	5.0	65.0	-	-	0.0259	0.0246	-	-
	Bu-grid2.5 exact	5.0	65.0	-	-	46	44	-	-
	ForLion	4.119	64.968	-	-	0.0253	0.0247	-	-
	ForLion exact grid2.5	5.0	65.0	-	-	45	44	-	-
	EW Bu-grid2.5	5.0	65.0	-	-	0.0255	0.0248	-	-
	EW Bu-grid2.5 exact	5.0	65.0	-	-	45	44	-	-
	EW ForLion	4.185	64.902	-	-	0.0251	0.0249	-	-
	EW ForLion exact grid2.5	5.0	65.0	-	-	45	44	-	-
17	Bu-grid2.5	17.5	142.5	145.0	-	0.0268	0.0015	0.0237	-
	Bu-grid2.5 exact	17.5	145	-	-	48	45	-	-
	ForLion	17.181	144.491	-	-	0.0265	0.0254	-	-
	ForLion exact grid2.5	17.5	145	-	-	47	45	-	-
	EW Bu-grid2.5	17.5	137.5	140.0	142.5	0.0266	0.0005	0.0193	0.0052
	EW Bu-grid2.5 exact	17.5	140	-	-	47	45	-	-
	EW ForLion	17.437	140.331	-	-	0.0262	0.0251	-	-
	EW ForLion exact grid2.5	17.5	140.0	-	-	47	45	-	-
18	Bu-grid2.5	17.5	20.0	92.5	95.0	0.0280	0.0042	0.0115	0.0176
	Bu-grid2.5 exact	17.5	20.0	92.5	95.0	50	7	23	29
	ForLion	17.157	19.653	93.331	-	0.0301	0.0019	0.0298	-
	ForLion exact grid2.5	17.5	92.5	-	-	57	53	-	-
	EW Bu-grid2.5	17.5	92.5	95.0	-	0.0312	0.0123	0.0159	-
	EW Bu-grid2.5 exact	17.5	95	-	-	56	50	-	-
	EW ForLion	17.933	94.525	-	-	0.0314	0.0282	-	-
	EW ForLion exact grid2.5	17.5	95.0	-	-	56	50	-	-

S5. Robustness of Sample-based EW Designs

In this section, we use the minimizing surface defects experiment (see Section 4.2) to illustrate the robustness of sample-based EW D-optimal designs against different sets of parameter vectors.

For illustration purpose, we simulate five random sets of parameter vectors from the prior distributions listed in Table S1 of Huang et al. (2024), denoted by $\Theta^{(r)} = \{\theta_1^{(r)}, \dots, \theta_B^{(r)}\}$, with $B = 1000$, and $r \in \{1, 2, 3, 4, 5\}$. For each $r = 1, \dots, 5$, we obtain the corresponding sample-based EW D-optimal design $\xi^{(r)}$ for the minimizing surface defects experiment, which maximizes $f_{\text{SEW}}(\xi) = |\hat{E}\{\mathbf{F}(\xi, \Theta^{(r)})\}| = |B^{-1} \sum_{j=1}^B \mathbf{F}(\xi, \theta_j^{(r)})|$. The numbers of design points are 15, 13, 21, 19, and 17, respectively.

For $l, r \in \{1, 2, 3, 4, 5\}$, we calculate the relative efficiencies of $\xi^{(l)}$ with respect to $\xi^{(r)}$ under $\Theta^{(r)}$, that is,

$$\left(\frac{|\hat{E}\{\mathbf{F}(\xi^{(l)}, \Theta^{(r)})\}|}{|\hat{E}\{\mathbf{F}(\xi^{(r)}, \Theta^{(r)})\}|} \right)^{1/p}$$

with $p = 10$. The relative efficiencies are shown in the following matrix

$$\begin{array}{c} \begin{matrix} l=1 & l=2 & l=3 & l=4 & l=5 \\ r=1 \\ r=2 \\ r=3 \\ r=4 \\ r=5 \end{matrix} \left(\begin{array}{ccccc} 1.00000 & 0.99179 & 0.99586 & 0.99284 & 0.98470 \\ 0.98258 & 1.00000 & 0.98508 & 0.98134 & 0.98117 \\ 0.99078 & 0.98748 & 1.00000 & 0.98165 & 0.98632 \\ 0.97629 & 0.98376 & 0.97910 & 1.00000 & 0.98501 \\ 0.97947 & 0.98850 & 0.98804 & 0.98842 & 1.00000 \end{array} \right) \end{array}$$

with the minimum relative efficiency 0.97629.

By applying the rounding algorithm (Algorithm 2) with merging threshold $L = 1$ and the number of experimental units $n = 1000$, we obtain the corresponding exact designs, whose numbers of design points are still 15, 13, 21, 19, and 17, respectively. Their relative efficiencies are

	l=1	l=2	l=3	l=4	l=5
r=1	1.00000	0.99144	0.99593	0.99299	0.98448
r=2	0.98287	1.00000	0.98535	0.98174	0.98128
r=3	0.99080	0.98716	1.00000	0.98184	0.98614
r=4	0.97634	0.98359	0.97916	1.00000	0.98488
r=5	0.97959	0.98836	0.98797	0.98846	1.00000

with the minimum relative efficiency 0.97634.

In terms of relative efficiencies, the sample-based EW D-optimal designs for this experiment are fairly robust against the different sets of parameter vectors.

S6. More Examples

In this section, we provide two more examples, including an electrostatic discharge experiment example and a three-continuous-factor artificial example, both under generalized linear models.

S6.1 Electrostatic discharge experiment

An electrostatic discharge (ESD) experiment was considered by Lukemire et al. (2019) and Huang et al. (2024), which involves a binary response, four discrete factors, namely LotA, LotB, ESD, and Pulse, all taking values in $\{-1, 1\}$, and one continuous factor Voltage in $[25, 45]$. The list of factors, corresponding parameters, the nominal values adopted by Lukemire et al. (2019), and the prior distribution adopted by Huang et al. (2024) are summarized in Table S.5. Lukemire et al. (2019) employed a d -QPSO algorithm and derived a locally D-optimal approximate design with 13 support points for a logistic model $Y \sim \text{Bernoulli}(\mu)$ with $\text{logit}(\mu) = \beta_0 + \beta_1 \text{LotA} + \beta_2 \text{LotB} + \beta_3 \text{ESD} + \beta_4 \text{Pulse} + \beta_5 \text{Voltage} + \beta_{34}(\text{ESD} \times \text{Pulse})$. Huang et al. (2024) used their ForLion algorithm and found a slightly better locally D-optimal design in terms of relative efficiency, which consists of 14 design points. Both designs were constructed under the assumption that the nominal values listed in Table S.5 are the true values.

In practice, however, an experimenter may not possess precise parameter values before the experiment. As an illustration, we adopt the prior distributions listed in Table S.5 (i.e., independent uniform distributions) on the model parameters. By applying our EW ForLion algorithm on the same model with the specified prior distribution, we obtain the integral-based EW D-optimal approximate design, and present it on the left side of Table S.6, which consists of 18 design points. Subsequently, we utilize our rounding algorithm with merging threshold $L = 0.1$ and the number of experimental units $n = 100$ (as an illustration) to obtain an exact design, and present it on the right side of Table S.6,

which consists of 17 design points (the 18th design point of the approximate design vanishes due to its low weight).

Table S.5: Factors and parameters for electrostatic discharge experiment

Type	Factor(Parameter)	Factor Levels/Range	Parameter Prior Distribution	Parameter Nominal Value
	Intercept(β_0)		$U(-8, -7)$	-7.5
Discrete	Lot A (β_1)	$\{-1, 1\}$	$U(1, 2)$	1.5
Discrete	Lot B (β_2)	$\{-1, 1\}$	$U(-0.3, -0.1)$	-0.2
Discrete	ESD (β_3)	$\{-1, 1\}$	$U(-0.3, 0)$	-0.15
Discrete	Pulse (β_4)	$\{-1, 1\}$	$U(0.1, 0.4)$	0.25
Continuous	Voltage (β_5)	$[25, 45]$	$U(0.25, 0.45)$	0.35
Discrete	ESD \times Pulse (β_{34})	$\{-1, 1\}$	$U(0.35, 0.45)$	0.4

Table S.6: EW D-optimal approximate design (left) and exact design (right, $n = 100$) for electrostatic discharge experiment

Support point							Support point	$N = 100, L = 0.1$					
	Lot A	Lot B	ESD	Pulse	Voltage	p_i (%)		Lot A	Lot B	ESD	Pulse	Voltage	n_i
1	-1	-1	-1	-1	25	8.48	1	-1	-1	-1	-1	25	8
2	-1	-1	-1	1	25	8.75	2	-1	-1	-1	1	25	9
3	-1	-1	1	-1	25	4.10	3	-1	-1	1	-1	25	4
4	-1	-1	1	1	25	8.56	4	-1	-1	1	1	25	9
5	-1	1	-1	-1	25	6.90	5	-1	1	-1	-1	25	7
6	-1	1	-1	1	25	5.15	6	-1	1	-1	1	25	5
7	-1	1	1	-1	25	9.01	7	-1	1	1	-1	25	9
8	-1	1	1	1	25	8.45	8	-1	1	1	1	25	8
9	1	-1	1	-1	25	7.43	9	1	-1	1	-1	25	7
10	1	1	-1	-1	25	3.56	10	1	1	-1	-1	25	4
11	1	1	-1	1	25	6.21	11	1	1	-1	1	25	6
12	1	1	1	-1	25	4.43	12	1	1	1	-1	25	4
13	1	1	1	1	25	0.90	13	1	1	1	1	25	1
14	-1	1	1	-1	38.948	7.94	14	-1	1	1	-1	38.9	8
15	-1	1	-1	-1	34.023	1.57	15	-1	1	-1	-1	34.0	2
16	-1	1	-1	1	35.405	3.80	16	-1	1	-1	1	35.4	4
17	-1	-1	1	-1	37.196	4.55	17	-1	-1	1	-1	37.2	5
18	-1	1	1	1	33.088	0.22							

To make comparison, we randomly generate $N = 10,000$ parameter vectors $\{\boldsymbol{\theta}_1, \dots, \boldsymbol{\theta}_N\}$ from the prior distribution listed in Table S.5. For each $j \in \{1, \dots, N\}$ and each $\boldsymbol{\xi}$ under comparison, we compute $(|\mathbf{F}(\boldsymbol{\xi}, \boldsymbol{\theta}_j)|^{1/p} = |\mathbf{X}_{\boldsymbol{\xi}}^T \mathbf{W}_{\boldsymbol{\xi}}(\boldsymbol{\theta}_j) \mathbf{X}_{\boldsymbol{\xi}}|^{1/p}$ with $p = 7$ in this case. In Figure S.3, we present the resulting values as frequency polygons for our EW ForLion design, the locally D-optimal design (“ForLion”) obtained by Huang et al. (2024), and the d -QPSO design (“PSO”) obtained by Lukemire et al. (2019). Compared with the ForLion or PSO design, the frequency polygon for EW ForLion design shows a slightly higher density with low objective functions values, but also a noticeably increased frequency in the higher-value range. Actually, in Table S.7, it clearly shows that the overall mean and median objective function values for EW ForLion designs (approximate and exact designs listed in Table S.6) are higher than ForLion and PSO designs.

S6.2 A three-continuous-factor example under a GLM

This example refers to Example 4.7 of Stufken and Yang (2012) on a logistic regression model with three continuous factors, represented as $\text{logit}(\mu_i) = \beta_0 + \beta_1 x_{i1} + \beta_2 x_{i2} +$

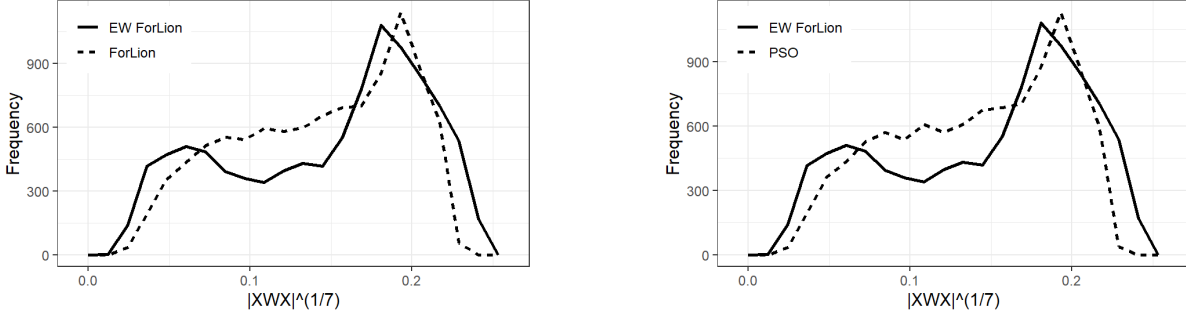


Figure S.3: Frequency polygons of objective function values based on 10,000 simulated parameter vectors for electrostatic discharge experiment

Table S.7: Mean and median objective function values based on 10,000 simulated parameter vectors for electrostatic discharge experiment

Design	Mean $ \mathbf{X}^T \mathbf{W} \mathbf{X} ^{1/7}$	Median $ \mathbf{X}^T \mathbf{W} \mathbf{X} ^{1/7}$
EW ForLion	0.14677	0.16422
EW ForLion exact	0.14676	0.16410
ForLion	0.14253	0.14990
PSO	0.14187	0.14878

$\beta_3 x_{i3}$, where the factors were originally defined as $x_{i1} \in [-2, 2]$, $x_{i2} \in [-1, 1]$, and $x_{i3} \in (-\infty, \infty)$.

In this section, for illustration purposes, we reconsider this example by letting $x_{i3} \in [-3, 3]$ and assuming independent priors $\beta_0 \sim N(1, \sigma^2)$, $\beta_1 \sim N(-0.5, \sigma^2)$, $\beta_2 \sim N(0.5, \sigma^2)$, and $\beta_3 \sim N(1, \sigma^2)$, with $\sigma = 1$. Using our EW ForLion algorithm, we obtain an EW D-optimal approximate design, which costs 783 seconds. We further apply our rounding algorithm to the approximate design with $L = 0.0001$ and $n = 100$, and obtain an exact design in just 0.45 second. Remarkably, both designs consist of 7 design points, as detailed in Table S.8, which are different from the 8-point design recommended by Stufken and Yang (2012) with unconstrained x_{i3} .

We compare our designs (“EW ForLion” and “EW ForLion exact-0.0001”) with EW D-optimal designs obtained by applying Bu et al. (2020)’s EW lift-one and exchange algorithms to grid points of continuous factors by discretizing them into 2, 4, 6, 8, and 10 evenly distributed grid points within the corresponding design regions. When the continuous variables are discretized into 10 evenly distributed grid points, Bu et al. (2020)’s EW lift-one and exchange algorithms no longer work due to computational intensity. The summary information of these designs are presented in Table S.9, from which we can see that our EW ForLion algorithm produces a design that is more robust against parameter misspecifications and also requires fewer design points.

Table S.8: EW D-optimal approximate design (left) and exact design (right, $n = 100$) for three-continuous-factor example

Support point	x_1	x_2	x_3	p_i (%)	Support point	x_1	x_2	x_3	n_i
1	-2	-1	-3	7.231	1	-2	-1	-3	7
2	2	-1	-3	20.785	2	2	-1	-3	21
3	-2	1	-1.8	19.491	3	-2	1	-1.8	19
4	2	1	3	2.718	4	2	1	3	3
5	2	1	-0.3321	18.870	5	2	1	-0.3321	19
6	-2	-1	-0.08665	10.951	6	-2	-1	-0.0867	11
7	0.94673	-0.99688	2.99323	19.954	7	0.9467	-0.9969	2.9932	20

Table S.9: Robust designs for three-continuous-factor example

Design	m	Time (s)	$ E\{\mathbf{F}(\boldsymbol{\xi}, \boldsymbol{\Theta})\} $	Relative Efficiency
EW Grid-2	7	0.06s	0.0009563	90.711%
EW Grid-2 exact	7	0.11s	0.0009559	90.700%
EW Grid-4	8	4.33s	0.0012320	96.641%
EW Grid-4 exact	10	5.03s	0.0012314	96.629%
EW Grid-6	8	13.87s	0.0013278	98.469%
EW Grid-6 exact	8	19.20s	0.0013271	98.455%
EW Grid-8	8	37.58s	0.0013562	98.989%
EW Grid-8 exact	9	46.42s	0.0013553	98.973%
EW Grid-10	-	-	-	-
EW Grid-10 exact	-	-	-	-
EW ForLion	7	782.05s	0.0014124	100.000%
EW ForLion exact-0.0001	7	0.45s	0.0014119	99.991%

Note: Relative Efficiency = $(|E\{\mathbf{F}(\boldsymbol{\xi}, \boldsymbol{\Theta})\}|/|E\{\mathbf{F}(\boldsymbol{\xi}_{\text{EWForLion}}, \boldsymbol{\Theta})\}|)^{1/p}$ with $p = 4$; “-” indicates “unavailable” due to computational intensity.